frontiers in Materials

REVIEW
published: 11 February 2022
doi: 10.3389/fmats.2022.848980

Recent Progress in Surface Modification of Mg Alloys for Biodegradable Orthopedic Applications

Shebeer A. Rahim[1], *M. A. Joseph*[1], *T. S. Sampath Kumar*[2]* *and Hanas T*[1,3]*

[1]Department of Mechanical Engineering, National Institute of Technology Calicut, Kozhikode, India, [2]Medical Materials Laboratory, Department of Metallurgical and Materials Engineering, Indian Institute of Technology Madras, Chennai, India, [3]Nanomaterials Research Laboratory, School of Materials Science and Engineering, National Institute of Technology Calicut, Kozhikode, India

The combination of light weight, strength, biodegradability, and biocompatibility of magnesium (Mg) alloys can soon break the paradigm for temporary orthopedic implants. As the fulfillment of Mg-based implants inside the physiological environment depends on the interaction at the tissue–implant interface, surface modification appears to be a more practical approach to control the rapid degradation rate. This article reviews recent progress on surface modification of Mg-based materials to tailor the degradation rate and biocompatibility for orthopedic applications. A critical analysis of the advantages and limitations of the various surface modification techniques employed are also included for easy reference of the readers.

Keywords: surface modification, magnesium alloys, biodegradation, orthopedic implant, biocompatibility, coating, pre-treatment

OPEN ACCESS

Edited by:
Changjiang Pan,
Huaiyin Institute of Technology, China

Reviewed by:
Jingxia Liu,
Southwest Jiaotong University, China
Thomas Webster,
Interstellar Therapeutics, United States

***Correspondence:**
Hanas T
hanas@nitc.ac.in
T. S. Sampath Kumar
tssk@iitm.ac.in

Specialty section:
This article was submitted to Biomaterials, a section of the journal Frontiers in Materials

Received: *05 January 2022*
Accepted: *18 January 2022*
Published: *11 February 2022*

Citation:
Rahim SA, Joseph MA, Sampath Kumar TS and T H (2022) Recent Progress in Surface Modification of Mg Alloys for Biodegradable Orthopedic Applications. Front. Mater. 9:848980. doi: 10.3389/fmats.2022.848980

INTRODUCTION

The use of ceramics and polymers showed early implant failure due to insufficient strength and instability (Zhao et al., 2017; Li et al., 2020a; Jahr et al., 2021). The metallic materials such as stainless steel, titanium, and cobalt–chromium based alloys were found to be superior to polymers and ceramics due to their mechanical properties. The Allied Analytics LLP analysis, 2021 predicts orthopedic implants as the highest income-generating segment among medical implants. However, when the implant is intended for a temporary application, they necessitate a second surgery. Also, the high elastic modulus of the metallic materials affects bone remodeling and leads to osteoporosis (Shi et al., 2021; Zhao et al., 2021). There were significant efforts to develop bioresorbable metallic implants for temporary orthopedic applications. The main advantage of such materials is that they avoid the additional surgical procedure to remove the implants after the tissue is healed (Qin et al., 2019; Luo et al., 2021). Such implants are expected to have mechanical properties close to human bone. The surface characteristics are expected to promote osteointegration and degrade at a rate compatible with tissue growth. The degradable implant can reduce the costs of health care and the chances for acquired infections due to repeated hospital visits (Khan et al., 2016; Dauwe et al., 2020; Herteleer et al., 2021; Xi et al., 2021). **Figure 1** summarizes the current limitations that can be addressed by developing a suitable biodegradable metallic material. Among the different metals available, Mg and Fe are among the most explored for degradable metallic implants. While Mg degrades much faster in the physiological environment, Fe alloys exhibit a very slow degradation rate.

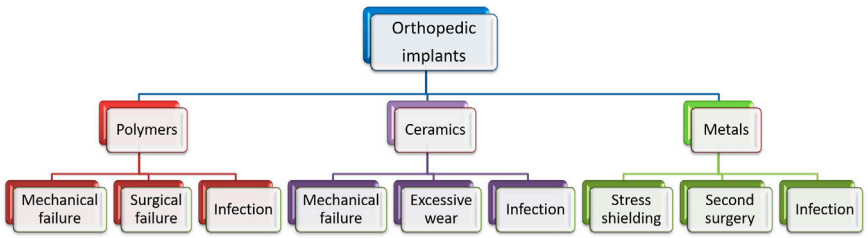

FIGURE 1 | Limitations of conventional materials for degradable orthopedic applications.

Both the high rate of degradation by Mg and the very slow degradation of Fe are not suitable for a degradable metallic implant. The degradation characteristic needs to be tailored to make it compatible with tissue growth. This article critically evaluates the surface modification techniques employed so far to tune the degradation rate of Mg alloys in the physiological environment.

Magnesium (Mg) is a biodegradable and lightweight metal with superior mechanical properties compared to polymeric and ceramic biomaterials. Also, the density and elastic modulus values are much closer to human bone, which is essential to minimize stress shielding and associated effects (Kirkland and Birbilis, 2014; Schumacher et al., 2019; Zhang et al., 2021b; Shang et al., 2021). Nevertheless, when exposed to human body fluid that contains corrosive ions like chlorides, the degradation process of Mg becomes more rapid and complex. Hence, after implantation, Mg alloys degrade rapidly, leading to loss of mechanical integrity before adequate growth of new bone tissue (Wang et al., 2020b; Rahman et al., 2020; Chandra and Pandey, 2021). Different metallurgical modification and surface modification techniques are reported for controlling degradation and enhancing the bioactivity of Mg surfaces in the physiological environment (Bryła et al., 2020; Heimann, 2021; Jahr et al., 2021).

Metallurgical modifications include optimizing microstructure and composition through alloying, composite fabrication, heat treatment, and plastic deformation processes. Although metallurgical modification effectively improves the mechanical properties and degradation resistance, the release of toxic alloying elements and contamination during such processes can cause detrimental effects to the neighboring tissues (Li et al., 2021b; Jiao et al., 2021). Also, metallurgical modifications are comparatively inefficient in promoting biocompatibility. In comparison, surface modification of Mg-based materials has a higher potential to control bioactivity and biodegradation in the physiological environment. Because the interactions between the physiological environment and implants start from the substrate surface, the biological response from the living tissue also depends on the surface features (Grzeskowiak et al., 2020; Jacob et al., 2020; Fong et al., 2021).

Surface modification is achieved by providing a protective coating or tuning the substrate surface morphology. The literature shows significant improvement in mechanical integrity, biodegradation, and biocompatibility of the Mg-based implants through various surface modification processes. The surface modification approach can be grouped into three major classes: chemical conversion coating, physical deposition coating, and surface microstructural modification.

CHEMICAL CONVERSION COATING

Conversion coatings are produced due to the electrochemical or chemical reaction of the Mg-substrate (Hughes, 2018). It is a cost-effective method that creates a protective superficial layer with better adhesion due to the chemical bond between the coating and Mg-substrate. A schematic representation is shown in **Figure 2**. The method involves wet-coating skills to generate a uniform layer to cover the entire substrate with different morphologies (Chen et al., 2015). Nevertheless, the relatively low durability and poor strength of these coatings limit the protection offered during prolonged applications under corrosive environments. However, these coatings can be used as a pre-treatment to form an adhesive base for deposition coatings (Jiang et al., 2019; Cheng et al., 2021). The major conversion coating techniques reported include electrochemical, acid, alkali, and hydrothermal treatments.

Electrochemical Conversion

The electrochemical conversion coating produces a protective layer on the Mg surface through electrochemical reactions (Luan et al., 2011; Liu et al., 2020). The added advantages of this method include low processing temperature, ease of controlling coating thickness, and coating complex shapes. The surface modification by electrochemical conversion of Mg-based materials falls into one of the following categories: anodization, electrodeposition (ED), electrophoretic deposition (EPD), and plasma electrolytic oxidation (PEO).

Anodization

During the anodization process, the Mg-substrate that acts as the anode gets oxidized, forming a protective oxide film on the surface. The formed coating generally has a nanostructured oxide layer with a thickness of up to 25 μm that can be controlled by changing anodization time, current density, and electrolytic concentration (de Oliveira et al., 2020; Mohan et al., 2020). Cipriano et al. (2017) performed anodization of pure Mg using 10 M KOH as the electrolyte at three different potentials (1.8, 1.9, and 2.0 V). A homogeneous microstructure and elemental composition were reported for 1.9 V. The anodized sample exhibited more than 50% reduction in I_{corr} and produced a passivation layer enriched with Ca and P. However, the Mg ion

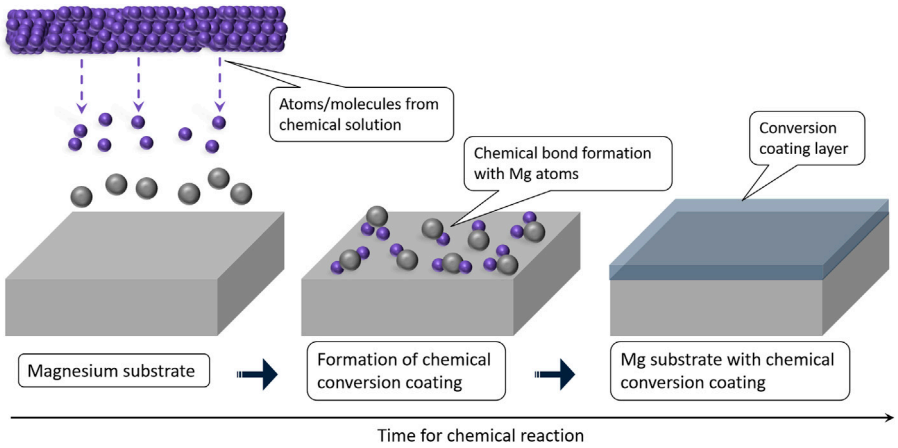

FIGURE 2 | Chemical conversion coating.

release for anodized samples was higher than that for the bare sample. Additionally, the anodized samples did not improve the cytocompatibility and proliferation of bone marrow cells. Rahman et al. (2019) investigated the effect of anodization as a function of time using alkaline electrolytes on AZ31 and ZK60 alloys. The results showed enhancement in electrochemical corrosion resistance and biocompatibility of coated samples due to the formation of anodized film containing MgO, $Mg(OH)_2$, and $MgCO_3$. The corresponding anodization time was 30 min at a voltage of 20 V. Zaffora et al. (2021) also found 30 min as the optimum anodization time corresponding to a current density of 20 mA/cm^2 and suggested that post-thermal treatment for 24 h at 350°C can enhance the corrosion resistance by one order of magnitude *via* sealing of the porous layers in the coating. Nevertheless, the hardness of oxide layers formed during anodization is poor, and the process is considered to be expensive.

Electrodeposition

ED is a simple and cost-effective method to develop a thin layer on the surface using an electrolyte that consists of material to be deposited. Song et al. (2010) obtained different types of apatite coatings (brushite, HA, and fluoridated HA) on Mg-6Zn alloy through ED, and the samples exhibited significant improvement in the degradation resistance. However, the degradation resistance was poor over a longer duration as the HA coating became fragile and unstable. Recently, Uddin et al. (2020) found that current density during the ED is crucial in controlling the HA coating characteristics. A lower current density of 3–6 mA/cm^2 produced regular and uniformly oriented HA crystals resulting in a micro-porous structure. A higher current density (13 mA/cm^2) resulted in randomly dispersed coarse crystals with non-uniform morphology. Coarsening the crystals reduced the effective surface area, leading to poor coating substrate adhesion. Also, the lower current density had a Ca/P ratio of 1.98, close to HA, and a higher Ca/P ratio was observed for increased current density. The corrosion rate of the samples decreased from 20.70 mm/year to 1.56 mm/year after coating with the lowest current density.

Wang et al. (2010) proposed pulse electrodeposition (PED), which could overcome the porosity associated with the applied static potential of the conventional method. The results showed better improvement in corrosion potential by 230 mV for as-cast Mg-Zn-Ca alloy without any post-treatment. Zhang and Lin (2019) reported a dense and homogeneous calcium stearate coating on AZ21 alloy through PED and found that the duty cycle has a significant effect in controlling coating morphology and the degradation rate. The anodized sample showed many cracks due to internal stress, while PED showed flower-shaped uneven protrusions of an average diameter of 24.4 µm on the coating. The diameter of flower-shaped protrusions decreased up to 12.8 µm with a decrease in the duty cycle and appeared finer and more homogeneous. The porous nanostructure significantly affected the wettability to obtain a superhydrophobic surface with a higher contact angle. Hamghavandi et al. (2021) studied the effect of PED process parameters and the composition of nanocomposite coating with chitosan and graphene oxide on the Mg-Zn scaffold with a porosity closer to that of bone. The best performance was obtained for a composition of chitosan with 2 wt.% GO when coated using a current density of 20 mA/cm^2 and a duty cycle of 0.5. The corrosion resistance improvement was noticed as a 120-mV shift in corrosion potential and reduction in corrosion current density by more than one order of magnitude. The MTT assay showed about 50% improvement in viability for L929 cells compared to the uncoated sample.

Electrophoretic Deposition

EPD is similar to ED, but the coating is not through the electrode reaction. During EPD, the charged particles dispersed in the electrolyte get deposited on the sample surface under the influence of an applied electric field. The concentration and zeta potential of the electrolyte were proven to be a deciding factor for obtaining a dense, crack-free, and uniform coating (Alaei et al., 2020; Saadati et al., 2021). The chitosan (CS) with bioglass (BG) coated on AZ91 alloys reported that the thickness and wettability of coating increased with concentration, and a lower concentration of 0.4 g/L BG produced a homogeneous and

compact coating morphology (Alaei et al., 2020). After the immersion test, the same coating concentration exhibited the best bioactivity by developing higher HA deposition on the surface. The Si-OH groups in the coating helped improve the wettability of the sample surfaces. However, the high deposition time associated with low and medium molecular weight CS produced coating discontinuities due to gas entrapment. Witecka et al. (2021) deposited high molecular weight CS/BG and CS/BG mixed with mesoporous nanosized BG on WE43 alloys. The high molecular weight CS reduced the deposition time to obtain a better coating morphology. The nano BG particles filled the spaces in between and improved the zeta potential. The modified composite coating also appeared more effective for improving cytocompatibility. However, compared to CS coating, both composite coatings exhibited a higher pH and weight loss due to the dissolution of BG particles. Askarnia et al. (2021) explored the antibacterial property of graphene oxide (GO) loaded with CS and HA on AZ91 alloy. The multiplication of both gram-negative *E. coli* and gram-positive *S. aureus* in the culture medium was reduced due to the antibacterial effect of GO. The antibacterial effect can be attributed to the ability of GO to penetrate bacterial cell membranes and wrap around the bacteria to inhibit bacterial proliferation (Zou et al., 2016).

Plasma Electrolytic Oxidation

The micro-arc oxidation, also called plasma electrolytic oxidation (PEO), is a high potential electrolytic process to generate plasma discharge, resulting in a robust and dense coating on the substrates that act as the anode. Initial work on PEO coating by Guo et al. (2006) showed that the developed porous ceramic coating comprised dense inner and outer porous layers. A relatively low voltage produces a fine porous structure, while the pore size increases for higher treatment times and voltages. The molten metal discharged through the pores act as a micro-arc discharge channel. However, cracks develop due to the induced thermal stress when the molten metal gets solidified. Zhang et al. (2020) reported improved degradation resistance and cell viability on MAO-coated AZ31 alloys. But with an increase in soaking time, the corrosive medium gradually penetrates the substrate surface through the micro pores. Wang et al. (2020d) produced a dense MAO coating with fewer cracks using a two-step current decreasing mode that decreased the corrosion rate from 0.9690 to 0.1559 g/m^{2}h during the immersion test in NaCl solution. Liu et al. (2021) suggested MAO as a pre-treatment for coating calcium metaphosphate (CMP) on AZ31B alloy. The MAO treatment shifted corrosion potential by about half and I_{corr} by more than one order of magnitude, and the pre-treatment resulted in the formation of minimum pits and defects on the degraded surface. After CMP coating, the corrosion potential shifted by 173 mV, and the I_{corr} was reduced to almost half that of the MAO pre-treatment. This significant improvement is due to the sealing of pores in the MAO-treated surface by the CMP coating. Zeng et al. (2016) conducted a biocompatibility test using fresh rabbit arterial blood and found an excellent reduction in the hemolysis ratio from 61.35 to 0.17% for the phytate–polylactic acid composite coated on MAO pre-treated Mg- 1Li- 1Ca alloy. The porous microstructure of composite coating (**Figure 3**) also enhanced the attachment of MC3T3-E1 cells. Peng et al. (2021) used Cu-containing electrolytes of different concentrations (0.1, 0.5, and 1 g/L) for MAO treatment of pure Mg. With the increase in Cu concentration, the coating was found to be denser, and the bacterial growth of *S. aureus* was inhibited by more than 50% due to the antibacterial effect of copper. However, higher concentrations (1 g/L) exhibited cytotoxicity with poor adhesion and proliferation of MC3T3-E1 cells. The findings suggest that Cu-doped MAO coatings with 0.5 g/L concentration can enhance the antibacterial property and control the rate of degradation.

Ghafarzadeh et al. (2021) also reported the modification of a porous MAO-treated surface into a smoother and uniform surface by electrospraying with poly-glycerol-sebacate. Wang et al. conducted EPD on ZK60 alloy to prepare an HA layer on the porous MAO coating and obtained a dense and uniform HA layer enclosing the micro-porous deposition (Wang et al., 2020c). Seyfi et al. (2021) investigated the effect of HA with various concentrations of ZnO (1–4 g/L) into the electrolyte during MAO. The coated samples showed an anodic shift of more than 800 mV and I_{corr} reduction by more than three orders of magnitude. Additionally, the anti-bacterial activity increased with ZnO concentration as the presence of Zn ions produces reactive oxygen species that attack the cell membrane of bacteria. Thus, it can be seen that porous MAO coating along with ceramic/polymeric coatings can enhance degradation resistance, bioactivity, and anti-bacterial property during prolonged immersion time.

Acid Treatment

Acid treatment is a cost-effective method to achieve a controlled degradation rate by treating the sample in acid solutions. The surface etching done by acid helps remove the surface contamination that occurred during the processing of metallic alloys. These contaminants, if not removed, cause micro-galvanic cells and promote corrosion on the substrate (Nwaogu et al., 2010). In addition, the thin films formed on the surface also help in passivation and thereby reduce the degradation. The treatment also helps in improving the surface energy favorable for cell adhesion and proliferation (Gawlik et al., 2019; Rahim et al., 2020). Mao et al. (2013) treated Mg–Nd–Zn–Zr alloy in 40% (vol.) hydrofluoric acid for 12 h to develop a protective magnesium fluoride (MgF_2) layer on the surface. Although the conversion coating improved degradation resistance, there was no significant improvement in cytocompatibility, and the hemolysis ratio was brought down from 52.0 to 10.1% only. Liu et al. (2019) obtained better corrosion resistance and biocompatibility for Mg-Sr alloy deposited with Ca ions and phytic acid treatment under a controlled pH level. The samples exhibited improvement in the *in vitro* behavior due to phosphoryl groups and Ca^{2+} ions on the coating, which supported HA formation. Similarly, Rahim et al. (2021a) reported improvement in biomineralization of Mg-Ca alloys by treating the samples with phosphoric acid and nitric acid. The formation of magnesium-phosphate and magnesium-hydroxide layers helps by providing a stable platform for nucleation and growth of HA

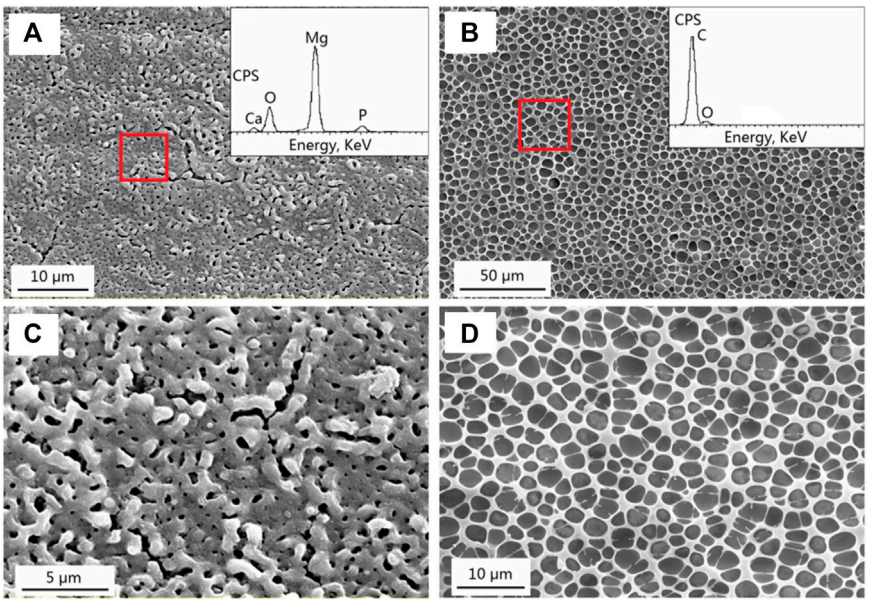

FIGURE 3 | SEM morphologies with EDS spectra; **(A)** MAO coating; **(B)** MAO/PLLA composite coatings on the Mg–1Li–1Ca substrate; **(C)** and **(D)** show higher magnification of **(A)** and **(B)**, respectively. Reprinted with permission from (Zeng et al., 2016), Copyright 2016, American Chemical Society.

on the sample surfaces. However, the stability of conversion coatings formed during acid treatment is a significant concern during long-term applications. Hence, acid treatment is preferable as a surface pre-treatment to improve the adhesion of subsequent deposition coatings.

Alkali Treatment

Like acid treatment, alkali treatment is also a simple chemical conversion coating method to produce a $Mg(OH)_2$ layer on the surface by treating it with a suitable alkaline medium (Saxena and Raman, 2021). Gu et al. (2009) compared the effect of different alkaline mediums, namely, disodium phosphate, sodium bicarbonate, and sodium carbonate, on Mg-Ca alloy. When treated with the alkaline mediums, the film formed on Mg-Ca alloy improved the degradation resistance without inducing any toxicity in L-929 cells. Among the alkaline mediums used, sodium bicarbonate showed the slowest degradation rate and maximum calcium deposition. Alkali treatment with different treatment times confirms that the film's thickness increases with an increase in treatment time (Tang et al., 2017). Wang et al. (2019b) reported improvement in corrosion resistance due to removing secondary phases from the surface by alkali-fluoride treatment on Mg-Zn-Y-Nd alloy. The *in vivo* test on the rat model substantiates uniform corrosion without any subcutaneous gas cavity formations. Li et al. (2020b) reported that the excess hydroxyl ions formed on the AZ31 alloys while treating them with NaOH acted as a corrosion barrier and promoted the reaction with vanillic acid treatment. However, like acid treatment, the stability of the conversion coating by alkali treatment is a crucial concern, and hence, they are better suggested as a pretreatment process.

Hydrothermal Treatment

Hydrothermal treatment is a simple, cost-effective coating technique to develop a coating on a metallic substrate. Xie et al. (2019) obtained a thin film of $Mg_5(CO_3)_4(OH)_2{\cdot}4H_2O$ particles with spherical flower-like morphology after 0.5 h of hydrothermal treatment in 0.5 M $NaHCO_3$. The film thickness increased with treatment time and finally obtained an irregular film of granular $MgCO_3$ and $Mg(OH)_2$ deposits after 3 h of treatment. However, hydrothermal treatment for 2 h showed better adhesion, and during the electrochemical corrosion test, the E_{corr} shifted to the nobler side by 343 mV and I_{corr} was reduced by one order of magnitude. Ali et al. (2021) prepared CaP coating on AZ31-3Ca alloy by single-step hydrothermal deposition using calcium nitrate (1 M) and diammonium hydrogen phosphate (0.6 M). The treatment was done at 100°C for 3 h and using two different pH values (4 and 7). **Figure 4** shows that the coated samples exhibited thick irregular-shaped plate-like depositions covering the substrate surface without any cracks. After immersion, unlike the bare samples, the treated samples developed thick depositions and protected the surface beneath. The coated samples exhibited a 60% reduction in degradation rate and a 65% reduction in H_2 evolution after 28 days of immersion. The coated samples retained more than 85% of the compressive strength after 14 days of immersion, while no measurable sample was left for the uncoated sample after 3 days to do the compression test. The cell culture study on MC3T3-E1 showed better cell attachment and cytocompatibility for both the coated samples. A similar approach was attempted before by Wang et al. (2019c), wherein Ca ions in HA were partially substituted with Sr ions. The addition of Sr resulted in forming a thin HA nanorod, and its microstructure changed from flower-like to a network-like structure. The compact morphology

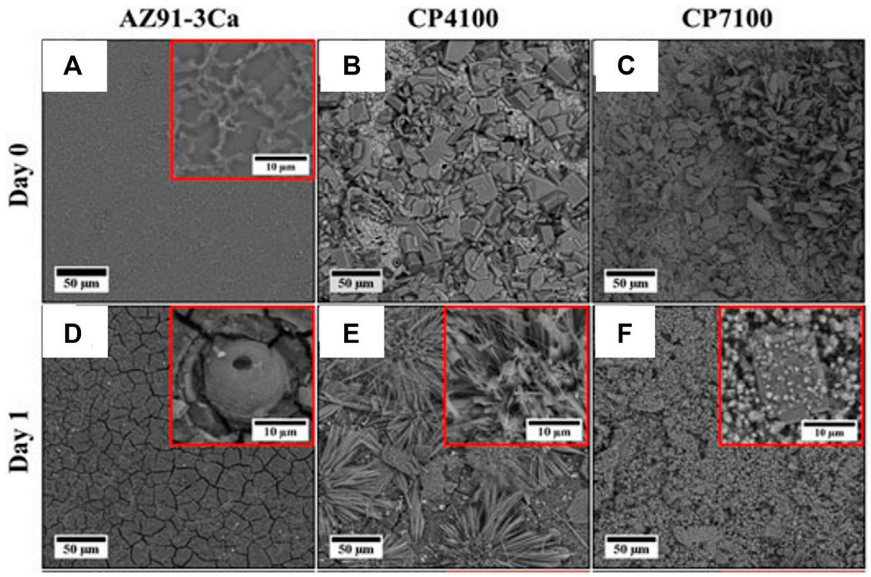

FIGURE 4 | SEM morphology before immersion; bare **(A)** coated samples at pH 4 **(B)** and at pH 7 **(C)** and their corresponding images after 1 day of immersion in SBF are **(D)**, **(E)** and **(F)** respectively. Reproduced with permission from (Ali et al., 2021), Frontiers.

TABLE 1 | Key findings from conversion coating methods.

Surface modification method	Key findings
Anodization	Develops a nanostructured oxide layer that can act as a scaffold for nucleation and growth of apatite and helps in reducing the degradation rate. The morphology and thickness of the anodized layer can be controlled by changing the process parameters and electrolytic concentration
Electrodeposition	Creates a porous microstructure with a characteristic morphology favorable for apatite formation. The poor degradation resistance over a prolonged duration of the porous microstructure can be overcome by using PED. The PED develops a homogenous porous nanostructure to enhance apatite formation and provide better resistance against degradation
Electrophoretic deposition	Develops a uniform and dense coating with better adhesion. The deposition formed can act as a stable scaffold to promote biomineralization. The incorporation of functional polymers or ceramics into the electrolyte can further enhance the bioactivity of EPD coating
Plasma electrolytic oxidation	Develops a robust coating with a dense inner layer and outer porous structure on the substrate. Secondary coating methods can be used to seal the porous structure to obtain improved degradation resistance and bioactivity
Acid and alkali treatment	Thin films obtained by reacting with a suitable acid or alkali medium can act as a scaffold for the nucleation and growth of apatite. Additionally, the etching caused during the chemical treatment removes the surface contaminations to inhibit micro-galvanic corrosion
Hydrothermal treatment	Develops thin films with characteristic morphology suitable for nucleation and growth of apatite. However, thin films developed by hydrothermal treatment as well as chemical treatments cannot withstand corrosive environments during prolonged immersion. Hence, they are suggested as surface pre-treatment methods

of Sr-doped coating can strongly hinder the contact between Mg substrate and the corrosive medium. Hence, Sr addition enhanced degradation resistance with improvement in cell adhesion and proliferation. Zhou et al. (2020) also obtained a high crystalline coating of nHA/ZnO on Mg bulk metallic glass that reduced the E_{corr} by more than 500 mV and the I_{corr} to a low value of 12.35 μA/cm^2. The presence of coated samples also produced an anti-bacterial rate of *S. aureus* and colon bacillus close to 100% due to the presence of ZnO. Similarly, the anti-bacterial effect was also reported by Li et al. (2021a), who developed a super hydrophobic HA/stearic acid composite coating on AZ31 alloy by hydrothermal treatment followed by treatment with stearic acid. The low surface energy inhibited the adhesion and growth of *E. coli* and *S. aureus* by entrapping the air layer in the nanostructured coating to reduce the contact between the surface and bacteria when exposed to the bacterial culture medium. The hydrothermal treatment was also reported as a pre-treatment to improve the adhesion of other surface coatings (Dilshad et al., 2019; Xi et al., 2020).

The conversion coating techniques are easy to execute and help in fine-tuning the surface microstructure. However, in cases such as acid or alkali treatment, the developed layers may not withstand the aggressive environment. The key findings from the conversion coating studies are listed in **Table 1**.

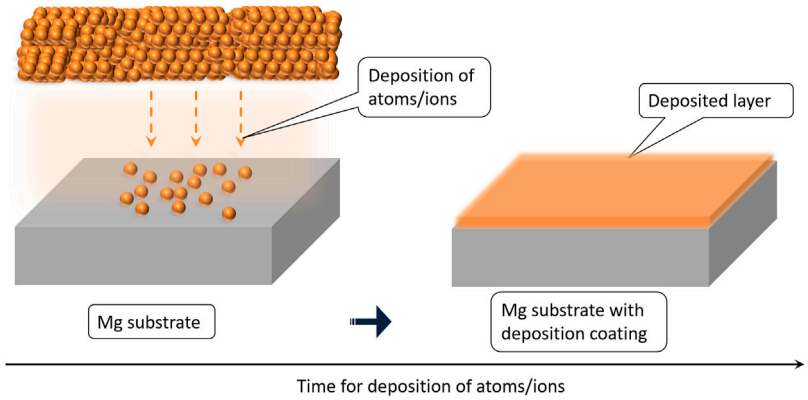

FIGURE 5 | Schematic representation of physical deposition coating.

PHYSICAL DEPOSITION COATING

Deposition coating techniques can also be used to develop a secondary layer on the substrate. The composition of such a layer can be easily tuned for imparting degradation resistance and better tissue implant interaction (Wang et al., 2012). The majority of these coatings reported are composed of CaP-based ceramic materials or biodegradable polymeric material (Saberi et al., 2021). The coating material is physically deposited on the Mg-substrate as schematically represented in **Figure 5**, and these coatings have better control on the degradation rate and bioactivity. However, the adhesion between the coating and the substrate is found to be inferior to the conversion coating in many cases (Wang et al., 2020a). The deposition coatings reported on Mg targeting for degradable implant applications include dip coating, spin coating, sol-gel coating, electrospinning, physical vapor deposition (PVD), chemical vapor deposition (CVD), and thermal spray coatings.

Dip Coating

The dip-coating method is suitable for coating complex shapes and relatively larger surfaces. The method allows the formation of functional polymeric or ceramic layers to act as a stable scaffold for promoting biomineralization and controlling the degradation (Guo et al., 2020; Rahim et al., 2021b). Abdal-Hay et al. (2012) dip coated poly vinyl acetate (PVAc) on AM50 alloy using dichloromethane, tetrahydrofuran, and N, N-Dimethylformamide as solvents. The coating developed using dichloromethane showed the highest adhesive strength (9.8 MPa), which was attributed to electrochemical bonding between PVAc and the substrate. The coating not only reduced the weight loss from 36.7 to 4.2 mg but also increased osteoblast viability by 30% on the first day and 50% on the third day of cell culture. Wang et al. (2019a) dip coated pure Mg rods with polyurethane (PU) functionalized with polyethylene glycol (PEG). The coating increased the degradation resistance, and the E_{corr} was reduced by 430 mV and the I_{corr} was reduced by two orders of magnitude. The coated samples also showed better resistance to *E. coli* bacterial adhesion due to the hydration barriers formed by the PEG chain. However, the use of the 2,2-dimethoxy-2-phenyl acetophenone catalyst reduced the L2 cell viability of PU coating from 85% to below 50% after PEG functionalization. Nikbakht et al. (2021) evaluated the performance of hydrofluoric acid pre-treatment followed by HA dispersed silane coatings on AZ31 alloy. The nano HA particles (size >200 nm) dispersed in silane coating enhanced degradation resistance by up to three orders of magnitude and improved cell proliferation. However, higher HA dispersion beyond 1,000 mg/L in the silane medium caused particle agglomeration to accelerate the degradation rate, as shown in **Figure 6**. Yang et al. (2021) coated Mg with a hybrid composite layer with a thickness of 1–2 μm using iron chloride hexahydrate dissolved in 20 ml de-ionized water. This method combined the conversion and the deposition process in a single step. The coating consisted of Fe along with $Mg(OH)_2$/MgO on pure Mg. The electrochemical measurement monitored continuously for 8 h in DMEM solution reported a large oscillation in E_{corr} between 200 and 1,200 mV due to the self-healing behavior after dip coating. Although the dip coating process is easy, controlling thickness and achieving the required coating adhesion are a major concern (Muñoz et al., 2020; Singh et al., 2021b). It is suggested that a proper surface pre-treatment and close control of process parameters are necessary to overcome the limitations.

Spin Coating

Spin coating appears to be a better method to deposit the biodegradable polymers due to its uniform coating thickness and better adhesion than dip coating. Spin coating biopolymers showed good adhesion onto the substrate with improved degradation resistance and cytocompatibility (Mousa et al., 2021; Zhou et al., 2021). Kozina et al. (2021) spin coated chitosan/water glass (CS/WG) on CaP-coated Mg-20Zn substrate. The CS-based coating hindered the corrosion for a longer immersion duration in Hank's solution. The

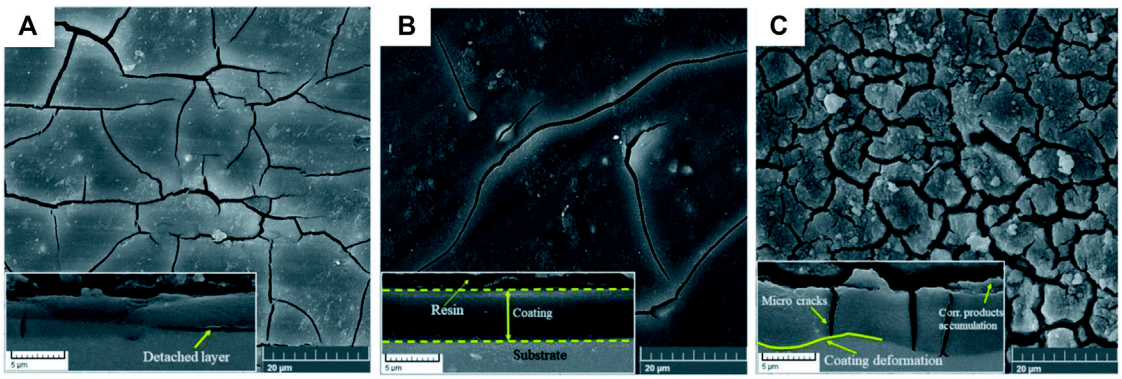

FIGURE 6 | Corrosion morphology with cross-sectional view (inset) after 1 week of immersion in SBF for different HA concentrations; **(A)** 500, **(B)** 1,000, and **(C)** 2,000 mg/L. Reproduced from (Nikbakht et al., 2021) with permission from the Royal Society of Chemistry.

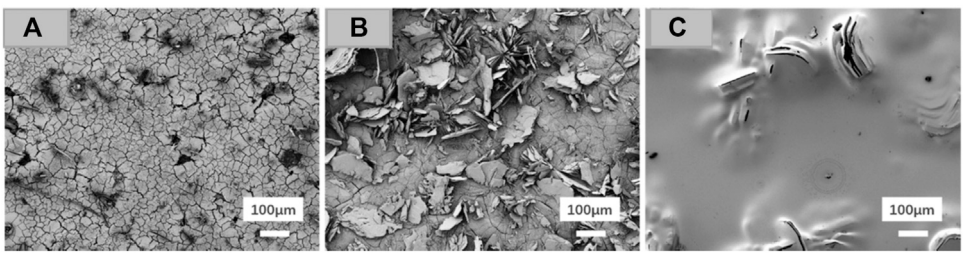

FIGURE 7 | SEM morphology after 72 h of immersion; **(A)** uncoated Mg, **(B)** pre-treated DAHP, and **(C)** spin coated DAHP/PEI60. Reprinted with permission from (Yang et al., 2019b), Copyright 2019, American Chemical Society.

degradation rate significantly decreased from 3.2 to 1.22 mm/year with a corresponding reduction in H_2 gas evolution. Yang et al. (2019b) spin coated polyether imide (PEI) on di ammonium hydrogen phosphate (DAHP). The coating reduced corrosion potential by more than 900 mV and corrosion current by five orders of magnitude. Unlike the typical cracked morphology observed for the bare samples, the composite spin coated samples exhibited a stable, smooth surface suitable for cell attachment, as shown in **Figure 7**. The cell distribution assessed by Vybrant Dil staining for pre-treated and spin coated samples showed higher density and better cell viability.

Zhao et al. (2018) developed multilayer polyvinylpyrrolidone/polyacrylic acid polymer coating using a novel layer by layer spin coating method and compared the performance with a similar dip coated multilayer sample. The coatings reduced corrosion current values from 1.63×10^{-5} to 3.11×10^{-6} and 9.89×10^{-7} A/cm^2, respectively, for dip coated and spin coated samples. Additionally, after immersion in HBSS, the spin coated samples had minor and smoother cracks with more Ca and P deposits on the surface. Kim et al. (2017) spin coated PLLA polymer on micro-patterned HA (by photolithography) to obtain a micro-textured HA/PLLA coating. The unique micro-texture obtained consisted of a periodic arrangement of crystallographic orientated needle-like HA crystals surrounded by PLLA. The coated samples exhibited excellent degradation resistance, biocompatibility, and high stability during mechanical strain. However, the spin coating method has limitations for larger surface areas.

Sol-Gel Coatings

The surface modification by sol-gel coating generates a thin layer of gel on the Mg surface dipped in a colloidal solution through polycondensation. Sol-gel dip coating is favorable for orthopedic applications as it utilizes low cost and low processing temperature to coat complex shapes using a wide range of materials (Figueira, 2020). Rojaee et al. (2013) prepared sol-gel–derived nHA coating using calcium nitrate tetrahydrate and phosphorous pentoxide as the precursors in ethanol. The coated AZ91 alloy exhibited a 100-mV anodic shift and reduction of I_{corr} from 22.14 to 2.83 µA/cm^2, as well as about three times increase in charge transfer resistance (R_{ct}). During the immersion test in modified SBF solution, the coating significantly reduced Mg ion release and maintained the pH value below 7.6 throughout the test. It may be noted that the concentration of the particles dispersed in the sol-gel is a critical parameter. Hernan et al. (2021) investigated different concentrations of functionalized graphene nanoplatelets (GNP) added to silica sol-gel *via* dip coating. The lowest GNP concentrations of 0.005–0.05 wt.% produced no visible defects or cracks. However, higher concentrations caused an increment in nanocharges of the sol-gel and changed the morphology. As a consequence of nanocharges, the viscosity was affected, and agglomeration of GNPs led to the formation of cracks

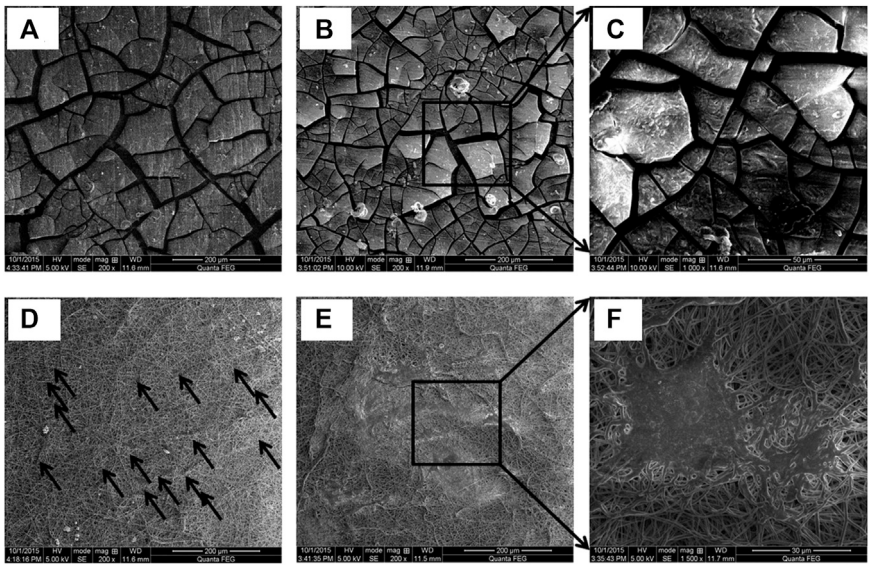

FIGURE 8 | Characteristic morphology of electrospun AZ31 alloy, after cell culture: **(A)** uncoated after 1 day, **(B)** and **(C)** after 3 days, **(D)** PCL/nHA composite coated after 1 day, and **(E)** and **(F)** after 3 days. Reprinted from (Hanas et al., 2018), Copyright 2018, with permission from Elsevier.

resulting in an irregular coating morphology. Although the higher GNP concentration will not affect cell proliferation, the cracked coatings may increase the degradation rate.

Omar et al. (2020) synthesized 58S and 68S bioactive silica glasses using the sol-gel method and dip coated on the AZ91D substrate. Although cracks were formed on the coatings, both coated samples produced excellent apatite formation from the third day of immersion. The coatings imparted enhanced corrosion resistance in Hank's medium, and the samples gradually degraded with time. The cell culture studies showed that the cells were well adhered, spread, and elongated for the coated samples. Su et al. (2018) reported HA and fluorine-doped HA sol-gel to seal porous CaP coating on AZ60 alloy by spin coating. The improvement in electrochemical corrosion resistance of the alloy after CaP coating further improved with sol-gel spin coating. During the immersion test in SBF, the H_2 gas evolution was reduced from 0.4 to 0.32 ml/cm^2 by CaP coating and was further reduced to 0.1 ml/cm^2 after the sol-gel spin coating. The coated sample also exhibited a reduction in pH from 10.5 to 8.5 after 7 days of immersion. (Kania et al. (2020) compared TiO_2 deposition *via* sol-gel spin and sputter coating. Compared with the bare sample, the spin coated substrate showed more than four times the reduction in H_2 gas evolution while sputter coating showed only a marginal reduction.

Electrospinning

Electrospinning utilizes electrical force to draw thin polymeric fibers onto the surface of the substrate and can be used to develop a coating on the surfaces which have a morphology similar to that of the extracellular matrix (Hanas et al., 2016; Rezk et al., 2019; Panahi et al., 2020). Panahi et al. (2020) electrospun PCL and PCL with nano BG on nitric acid pre-treated AZ91 alloy. After immersion in SBF, irregular deposits were observed for uncoated samples, while coated samples exhibited characteristic cauliflower-like morphology. Hanas et al. (2018) prepared PCL/nHA composite coating on nitric acid pre-treated AZ31 alloy by electrospinning. The results indicate that the extracellular morphology of electrospun fibrous PCL/nHA coating acted as a stable scaffold for accelerated biomineralization. The degradation rate of the coated samples was less than half of that of the uncoated samples throughout the immersion test. Furthermore, the L6 rat cells showed excellent cytocompatibility with significant improvement in percentage cell viability by more than 50%. Additionally, the uncoated sample exhibited poor cell adhesion, while the cells flattened and expanded on the composite coated sample due to the characteristic coating morphology, as shown in **Figure 8**. Perumal et al. (2020) prepared a bilayer coating of PCL/nHA by dip coating followed by electrospinning on an AZ31 cage implant and studied the *in vivo* behavior of New Zealand white rabbits. The *in vivo* test results showed enhanced bone healing and controlled biodegradation of the implant at the diseased site.

Karthega et al. (2021) electrospun coated PCL and PCL/nano TiO_2 with different TiO_2 compositions (2, 4, and 6 wt.%) on AM50 alloy. A higher concentration of nano TiO_2 increased the fiber diameter due to the increased viscosity of the spinning solution that favors the degradation resistance. The composite coating with 6 wt.% nano TiO_2 reduced E_{corr} from 1.45 V to well below 0.5 V and I_{corr} by more than four orders of magnitude. The distribution of L929 cells was also more uniform for the composite nano-fiber coating. The electrospinning PLLA incorporated with GO and Ag-NP on Mg-1Ca-3Zn alloy also improved the degradation resistance and bioactivity of Mg alloys (Bakhsheshi-Rad et al., 2020). The anti-bacterial resistance of bare and PLLA coating was significantly enhanced after the addition of GO. The inhibition zone for *E. coli* and *S. aureus*

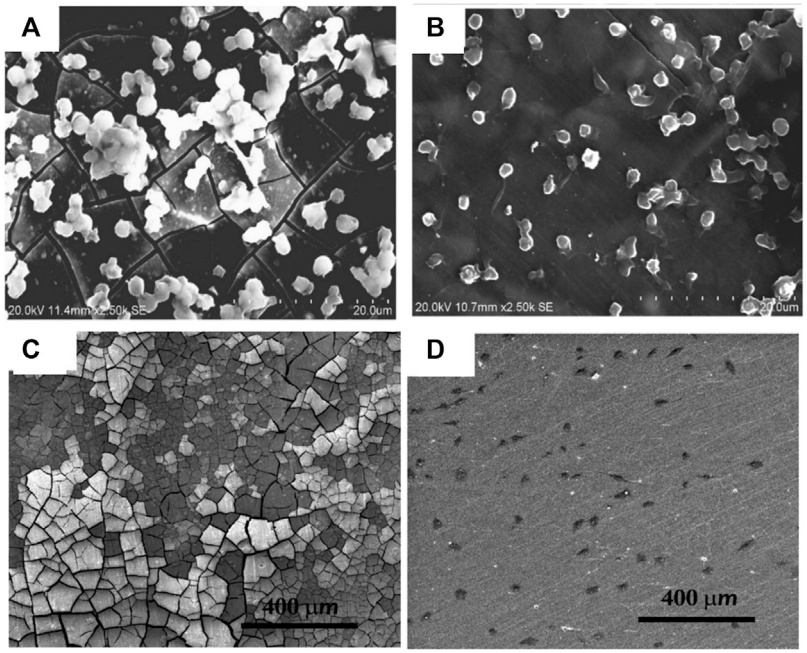

FIGURE 9 | Morphology of adherent platelets in **(A)** bare, **(B)** TiO_2-coated MgZn substrate, and Ea. hy 926 cells cultured after 1 day, **(C)** bare and **(D)** TiO_2 coated. Reproduced with permission from (Hou et al., 2020), MDPI.

growth was doubled after the addition of Ag-NP. The oxygenated groups in GO facilitate the homogeneous release of Ag + ions to cause bacterial destruction. Bakhsheshi-Rad et al. (2019) also reported excellent improvement in degradation resistance and anti-bacterial property for PCL/MgO-Ag electrospun on tantalum pentoxide sputter coated Mg-Ca-Zn alloy. However, incorporating a higher amount of particles can reduce the degradation resistance as the electrospun fibers become rough with reduced diameter.

Physical Vapor Deposition

PVD is a coating technique that physically deposits atoms or ions onto the substrate to yield a highly adhesive and uniform coating. Sputtering, thermal evaporation, and ion plating are the different types of PVD.

Sputter Coating

Sputter coating utilizes plasma to eject atoms toward the Mg target under a high vacuum. Surmeneva et al. (2015) prepared an HA target for sputter coating on Mg-Ca alloy and developed a coating of a thickness well below 1 μm. The HA coating reduced the corrosion current from 90 to 1.8 $\mu A/cm^2$ and polarization resistance by more than two orders of magnitude. The HA was also sputter coated in AZ91 alloy with a substrate bias of −25 V and −100 V, followed by annealing treatment (Surmeneva et al., 2019). The application of higher negative bias on the substrate improved the surface morphology to enhance the adhesion of bone marrow stromal cells. However, samples annealed post-deposition showed cracks causing rapid degradation and poor cell adhesion. Hou et al. (2020) reported excellent anti-hemolytic property and cytocompatibility for TiO_2 sputter coating. The hemolysis ratio of MgZn alloy was significantly reduced from 47 to 0.1% after TiO_2 sputter coating. It is reported that micro-cracks in the uncoated alloy resulted in platelet aggregation that can cause thrombosis, while the coated samples showed good surface morphology and no platelet agglomeration, as shown in **Figures 9A,B**. Furthermore, the coated samples showed cell viability above 90% with excellent cell adhesion and spindle-shaped proliferation as shown in **Figures 9C,D**.

The addition of Sr to CaP while sputter coating two different rare earth Mg alloys was reported by (Acheson et al., 2021). Although Sr-CaP sputter coating dissolved during the immersion test, the degradation rate of the samples reduced by almost 30%. Yasakau et al. (2021) sputtercoated Mg5Gd alloy pins using the same material as the source. The SEM micrographs showed an independent columnar growth perpendicular to the alloy pin surface without coalescence. During immersion in HBSS, the characteristic columnar growth protected the coated sample with dense CaP deposits and reduced the degradation rate by ten times. Levent et al. (2019) sputter coated Ag-based bioceramics on MAO pre-treated AZ31 alloy. The sputter coated samples exhibited super-hydrophobicity with more biomineralization deposits homogenously dispersed than those of the uncoated samples. Additionally, the anti-bacterial effect of Ag in sputter coated samples reduced the active colony ratio of *E. coli* and *S. aureus* by 87 and 74%, respectively, compared to that of MAO pre-treatment. Sputter coating with the same composition as that of the Mg-substrate is suggested to have a higher potential for biodegradable implants (Yasakau et al., 2021).

Thermal Evaporation

The selected coating material is vaporized by heating and then allowed to deposit on the substrate in the thermal evaporation process. Wang et al. (2018) compared the degradation performance of Mg foam subjected to thermal evaporation and thermal diffusion. Both the coatings improved the compressive strength and elastic modulus by more than 70%. The Zn-based deposition during thermal evaporation had a smooth and dense texture with strong interface bonding that acted as a barrier and improved the degradation resistance of Mg-foams. However, the thermal diffusion method exhibited accelerated corrosion due to the galvanic effect of Mg-Zn along the grain boundaries. After 6 days of immersion in SBF, pH and weight loss were reduced from 9.79 to 7.88 and from 15.17 to 2.19%, respectively, for Zn deposited by thermal evaporation. Calderón et al. (2021) reported that deposition of the $Mg_{17}Al_{12}$ intermetallic phase by thermal evaporation of Al on pure Mg and AZ31B alloy improved degradation resistance. However, a detailed investigation on the biomineralization and other biological surface activities on the surface coated using thermal evaporation is necessary.

Ion Plating

PVD by ion plating combines the principle of thermal evaporation and sputtering for depositing ions on the substrate surface. Ba et al. investigated the effect of Mg-Al hydrotalcite, Zr_2ON_2 and Mg-Al hydrotalcite/Zr_2ON_2 coating on Mg-Gd-Zn alloy (Ba et al., 2016). The surface morphology of coatings showed that ion plating is uniform and a crack-free surface can be obtained. The PDP and Nyquist plots revealed enhancement in corrosion resistance for coated samples, which can be attributed to the passivation by the composite layer. The preclinical or clinical studies on ion plating of Mg-based materials are worthwhile to investigating biocompatibility. Also, during prolonged immersion, there is a higher chance that Mg-substrate may get exposed to the corrosion medium due to delamination of PVD coatings. Hence, prolonged studies need to be conducted for these cases.

Chemical Vapor Deposition

During the CVD process, volatile precursors can react with the Mg surface to obtain thin films and coatings. Although CVD coating demands high initial investments, it offers a controllable deposition rate to obtain uniform thickness for complex geometries. Chen et al. (2019b) deposited MgO/MgF_2 composite coating on porous Mg samples and obtained more than 50% reduction in H_2 gas evolution. The electrochemical test also significantly reduced E_{corr} by more than 300 mV and I_{corr} by more than one order of magnitude. Since the composite coating has limited solubility in SBF, they acted as a barrier and blocked contact with the substrate to prevent rapid corrosion. However, with the increase in immersion time, SBF passes through the coating's pinhole defects, leading to substrate corrosion. Yang et al. (2019a) prepared carbon nitride film on AZ31B alloys with urea as the precursor at three different temperatures. The corrosion potential of coated samples shifted to the noble side by more than 275 mV, and charge transfer resistance improved by two orders of magnitude. Apart from improving electrochemical corrosion resistance, during the early stage of immersion in SBF, the coated samples only had a little H_2 evolution while the uncoated sample exhibited uncontrolled release. Even though coating deposited at different temperatures yielded similar degradation resistance, biocompatibility studies suggest 450°C as the preferred processing temperature for carbon nitride coating on AZ31B alloys. However, delamination and contamination of the CVD deposits should be carefully evaluated to propose this technology for biomaterials.

Atomic Layer Deposition

ALD is a unique technique under the subclass of CVD for growing thin films with precise thickness and composition. Yang et al. (2017) fabricated zirconia nanofilm with different process cycles (100, 200, 300, and 400) on Mg-Sr alloy by ALD. The size of the uniformly deposited nanoparticles decreased with an increase in the number of cycles. The electrochemical corrosion test results showed anodic shift for E_{corr} and a decline in I_{corr} values with increased process cycles of the zirconia-coated samples. The EIS results and immersion test results also substantiated the above findings. Additionally, the stable, biocompatible zirconia layer significantly improved the cell viability by more than two times and ALP activity by more than 40% of that of the control. The fluorescent microscopy images and SEM morphology conclude that coating favors cell proliferation while the corrosion cracks of the uncoated sample break the cells. Peron et al. (2020), Peron et al. (2022) also obtained better results for zirconia than titania deposition on AZ31 alloy during ALD. Titania coating reduced I_{corr} by two orders of magnitude and H_2 evolution by 53%, with cytotoxicity decreasing from grade 1 to grade 2. However, zirconia reduced coating I_{corr} by three orders of magnitude and H_2 evolution by 92% while maintaining grade 1 cytotoxicity. The slow strain rate fractography studies conducted in SBF showed that the coated samples developed fewer cracks than bare samples, though the zirconia-coated samples exhibited necking, as shown in **Figure 10** (Peron et al., 2020).

Thermal Spray Coating

Besides the methods mentioned above, biodegradation and bioactivity of Mg-based materials are modified by coating metallic and non-metallic materials by different thermal spray processes. Mardali et al. (2019) deposited micro-HA particles on AZ61 alloys using the high-velocity oxygen fuel (HVOF) spray method. Compared to conventional thermal spray, the HVOF method produced micro-cracks on the coating to obtain an open-pore structure for improving cell adhesion. The higher quantity of HA crystalline phases decreased H_2 evolution by more than 85% and increased charge transfer resistance by more than one order of magnitude. However, a gradual loss in degradation resistance occurred over time due to the leakage of SBF solution into the substrate through micro-cracks. Singh et al. (2019) attempted plasma spray coatings using HA, Nb, and HA/Nb to improve the degradation resistance and biocompatibility of ZK60 alloys. The

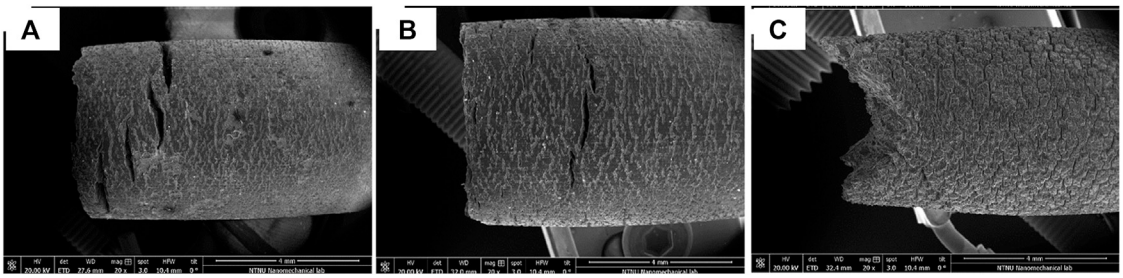

FIGURE 10 | SEM fractography of the gauge section of AZ31 samples after slow strain rate tests in SBF; **(A)** bare, **(B)** titania coated, and **(C)** zirconia coated. Reproduced with permission from (Peron et al., 2020), Elsevier.

TABLE 2 | Key findings from physical deposition coating methods.

Surface modification method	Key findings
Dip coating	The method develops functional polymeric or ceramic layers around substrates of any geometry. The developed layer acts as a scaffold to promote biomineralization and protects the surface against corrosion. A suitable pretreatment is suggested before dip coating to enhance adhesion to the substrate
Spin coating	Develops biodegradable polymer coatings with uniform thickness on a flat substrate surface. Spin coated samples have better adhesion and can remain as a stable scaffold for a prolonged duration. Multilayer coatings can also be developed to obtain enhanced protection of the substrate
Electrospinning	Deposits polymeric or composite fibers on the substrate surface with coating morphology similar to that of the extracellular matrix. The characteristic morphology can significantly improve degradation resistance and enhance apatite formation with excellent cell attachment
Sputtering	Deposits atoms from metallic and non-metallic materials into the substrate surface to develop a thin coating with controllable morphology. The developed coating with a thickness less than 1 μm can act as an excellent corrosion protection barrier
Thermal evaporation and ion plating	Deposits atoms or ions into the substrate surface. The dense texture and excellent interface bonding of the deposited layer act as an excellent barrier against degradation
Chemical vapor deposition	Develops uniform coating with a controlled thickness on complex geometries. The coating acts as a barrier and protects the substrate from the surrounding medium. However, the PVD and CVD coatings can delaminate during prolonged immersion
Thermal spray	Deposits metallic and non-metallic materials using different thermal spray coating methods. The micro-cracks formed during the thermal spray method act like an open-pore structure to facilitate cell adhesion. However, the corrosive medium can penetrate through the cracks during prolonged immersion

coatings caused slight shifting of corrosion potential to the nobler side with three to four times reduction in the corrosion current density. However, only HA coating and Nb-reinforced HA coatings showed hydrophilicity and a hemolysis ratio of less than 5%. Bansal et al. (2020), Bansal et al. (2021) reported that plasma spray coating of HA with Sr and ZnO improved the degradation resistance of Mg alloys. Incorporating reinforcing particles into the HA increased the coating microhardness significantly to prevent rapid deterioration and impart load-bearing capacity during implant applications. The characteristic nanostructure obtained by sealing the pores of the PEO layer by ZrO_2 plasma spraying reduced E_{corr} by more than 600 mV and I_{corr} by more than three orders of magnitude (Daroonparvar et al., 2018). Also, the anti-bacterial study in *E. coli* bacteria shows an increase in the inhibition zone diameter from 1.2 to 2.5 mm after coating due to the accumulation of nano ZrO_2 in the bacterial membrane and cytoplasmic areas (Gowri et al., 2014). Daroonparvar et al. (2020) obtained improved wear and degradation resistance with excellent bioactivity during cold spraying of hard Ti and Ta/Ti coating on AZ31 alloys. Ti coating improved Rct by two orders of magnitude, whereas Ta/Ti coating improved R_{ct} by four orders of magnitude. In addition to the passivating nature of the coatings, the rough island-like coated surface acted as nucleation sites for CaP formation in HBSS.

The physical deposition coating methods help in providing the required composition and morphology for the surface. However, in many cases, a proper pre-treatment is often necessary before the deposition coating to ensure proper adhesion between the substrate and the coating. The key finds from deposition methods are included in **Table 2** for easy reference.

SURFACE MICROSTRUCTURAL MODIFICATION

Surface microstructural modification is an alternate approach to tune the degradation and bioactivity of biometals. Such methods reported so far combine the effect of grain refinement and compressive residual stress developed near the surface for changing the surface morphology of the Mg-substrate (Zhang et al., 2019b, Zhang et al., 2021a; Singh et al., 2021a). The surface metallurgical modification achieved is schematically represented in **Figure 11**. The modification has a significant

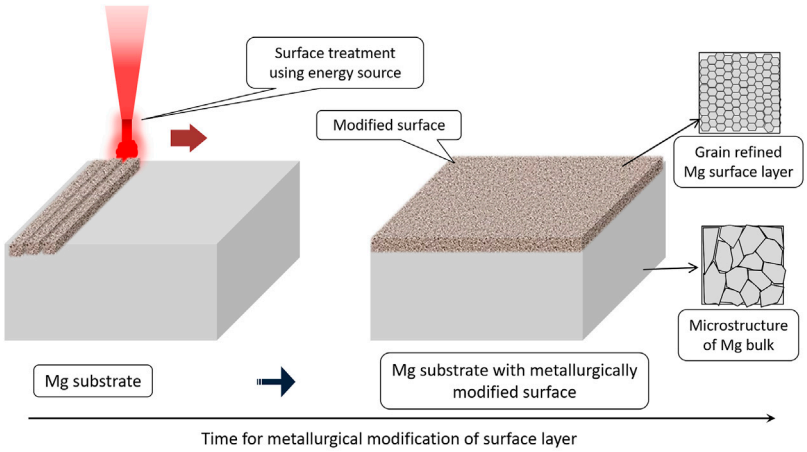

FIGURE 11 | Surface metallurgical modification.

impact on the surface wettability of Mg and could strongly influence biodegradation and bioactivity during implant applications (Lu et al., 2019). However, most surface microstructural modification methods investigate surface mechanical properties and wear behavior. Hence, it is necessary to further investigate the possibility of such methods from a biological perspective.

Pulsed Electron Beam Treatment

The method utilizes a PEB that rapidly melts and then quenches the Mg-substrate to create metallurgical modification on the surface and subsurface region while the bulk of the substrate material is not affected by the treatment. In addition to controlling the degradation rate, PEB can significantly improve the surface mechanical properties. Gao et al. (2007) reported the formation of a protective nano-grained MgO layer on AZ91 alloy. Beneath the MgO layer, a molten layer of Al over super-saturated α-Mg was formed by solute trapping. The modified layer favored passive film formation and reduced the degradation rate by two times. However, the rapid melting and solidification of the AZ91 alloy surface produced crater defects with secondary phase eruption. Lee et al. (2020) also observed selective removal of pre-existing precipitates in the PEB modified layer that reduced H_2 evolution from 5.8 to 2.8 ml/cm^2 and weight loss from 12 to 6.5 mg/cm^2. In addition to forming a protective layer, removing impurities and grain refinement can also promote degradation resistance (Lee et al., 2019). Morini et al. (2021) surface-treated AZ91 and AM60 alloys using low-energy high-current PEB through different acceleration voltages (15–30 kV) and a high number of pulses (up to 100). Although the process resulted in Al enrichment on the layer modified by PEB increasing the Vickers microhardness value by more than two times, there was no significant improvement in the electrochemical corrosion test using 3.5 wt.% NaCl solution. Furthermore, detailed *in vitro* degradation and cytotoxicity investigations are necessary to understand PEB-treated Mg-based materials' degradation behavior for implant applications.

Laser Surface Melting Treatment

Like electron beam treatment, LSM uses laser heat to modify the Mg surface, while the latter has a better controllable nature and excellent repeatability. LSM creates intense microstructural changes with fine dendritic grain formation to a controllable level of depth without significant porosity. The extent of the modified layer depends on the LSM process parameters such as scan speed, laser power, and spot size. Wu et al. (2021) explored LSM on microstructure and surface texture evolution in AZ31B alloy. The high thermal gradient during the treatment led to predominant prismatic crystallographic texture along the *Z* direction. Concurrently, grain growth in the same direction led to the formation of a cellular/dendritic microstructure with uniform distribution of $Mg_{17}Al_{12}$ phase along the grain boundaries. The LSM also produced rougher surfaces to enhance surface energy. The fine grain boundaries acted as nucleation sites for HA formation, and the Ca/P ratio of biomineralization product was 1.68. The characteristic microstructure also exhibited uniform corrosion due to the homogeneous distribution of the intermetallic phase that acted as a corrosion barrier (Wu et al., 2017). Zhang et al. (2019a) investigated the effect of melting and surface texturing during LSM on degradation of Mg-Gd-Ca alloys. The periodic surface textures enhanced mechanical properties and the degradation resistance. The cytocompatibility of untreated samples was significantly improved due to the attachment and proliferation of cells along the direction of LSM-induced nanotexture. Chopra et al. (2021) reported that the nanotexturing achieved on the implant surface could act like a "bed of nails" against bacterial growth while promoting bioactivity. However, at higher scanning rates, small cracks are formed due to the thermal stress during rapid cooling of the laser-melted zones (Guan et al., 2009). Lu et al. (2019) also observed grain refinement leading to an increase in secondary phase distribution on the Mg-substrate and consequently improving the wettability and degradation resistance. Guo et al. (2021) obtained improved cell viability and cell–cell connectivity for laser-treated surfaces due to their low degradation and higher surface energy. Rakesh et al., 2019

TABLE 3 | Key findings from surface metallurgical modification methods.

Surface modification method	Key findings
Pulsed electron beam treatment	Creates a protective nano-grained layer on the surface due to rapid melting followed by quenching. The layer improves degradation resistance due to the passive layer formation and eruption of impurities. However, the crater defects due to rapid melting and solidification can affect the degradation resistance
Laser surface melting	Develops a characteristic cellular/dendritic non-porous microstructure with uniform distribution of the intermetallic phase along the grain boundaries. The fine grain boundaries act as nucleation sites for biomineralization and the intermetallic phase acts as a corrosion barrier. The excellent repeatability and controllable nature of the method can be utilized to tailor the wettability of the substrate
SMAT and shot peening	The process produces a nanocrystalline surface-induced compressive residual stress, resulting in excellent surface mechanical properties and wear resistance. However, the higher surface roughness and surface contamination during the process are detrimental for biodegradable implant applications
LSP	The use of a laser enables better control over surface microstructure and residual stress. The fine grain refinement accelerates passive layer formation to enhance the degradation resistance

obtained improved degradation resistance with controlled pH increase for higher laser power and energy density. Manne et al. (2018) performed LSM on Mg-2.2Zn alloy using different laser powers and scanning speeds. The most refined microstructure corresponds to a power of 125 W and a scanning speed of 30 mm/s. They reported a decrease of more than 40% in the corrosion rate in HBSS and improved biomineralization due to surface energy enhancement for the LSM-treated substrate. Optimized LSM process parameters are essential to control the microstructure for improving cytocompatibility and degradation resistance. Furthermore, *in vivo* and *in vitro* study reports on LSM are limited to making a conclusive statement.

Surface Mechanical Attrition

SMAT is a severe plastic deformation process to introduce compressive residual stress into the Mg surface without affecting the microstructure of the bulk. The repeated impact of the substrate surface during the process with flying balls from different directions produces a hard nanocrystalline layer due to twinning and dynamic recrystallization and sub-grain formation (Showron et al., 2020; Singh et al., 2021a). Laleh and Kargar (2011) found enhancement in ultra-fine grain refinement and the microhardness value for AZ91D alloy irrespective of the ball size, which varied from 2 to 5 mm in diameter. However, the corrosion rate and depth of the nanocrystalline layer increased with the ball diameter due to the increased defect density. Li et al. (2014) obtained an extraordinary increase in H_2 evolution and a higher pH value for pure Mg and Mg- 1Ca alloys after SMAT. This decline in degradation resistance is because of the increased crystalline defect density after ultra-fine grain refinement. In a similar study, Chen et al. (2019a) also observed that SMAT decreases the degradation resistance of AZ31 alloy due to an unusual increase in the surface roughness. After SMAT, the H_2 evolution, weight loss, and the corresponding corrosion rate doubled. The electrochemical corrosion test also showed similar results, with larger balls having the highest corrosion rate. Additionally, the degradation resistance of SMAT samples deteriorates due to surface contamination arising from the attrition balls and the processing chamber (Showron et al., 2020). Thus, it can be seen that the use of SMAT for biodegradable applications of Mg-based alloys is less effective. Hence, it is suggested that SMAT may be considered as a pre-treatment technique and needs to be combined with a proper surface coating technique.

Shot Peening

Shot peening also introduces compressive residual stress into the Mg surface using a similar principle to SMAT. However, shot peening uses comparatively smaller balls to project into a fixed substrate with a higher velocity. Mhaede et al. (2014) observed that shot peening was an effective pre-treatment method to improve micro-hardness and degradation resistance. However, shot peeing unaided by coating deteriorated degradation resistance with a considerable drop in the polarization resistance. Yao et al. (2021) obtained excellent results for shot peening AZ91 alloys after zinc coating. The shot peening as post-processing improved the compactness of Zn coating with excellent improvement in microhardness and corrosion resistance. Compared to the bare sample, the H_2 evolution and weight loss were reduced by three times and ten times for the shot-peened Zn-coated samples. Peral et al. (2020) reported that higher surface roughness during shot peening contributes to the rapid degradation. Also, the detailed study focusing on the biological performance of different types of shot-peening did not yield satisfactory results. Bagherifard et al. (2018) observed higher I_{corr} values with no significant improvement in cell viability for different shot-peened samples. The above discussions suggest that shot peening can be considered a promising surface treatment method when used with deposition coatings as a pretreatment or post-treatment process.

Laser Shock Peening

Surface treatment using the laser shock peening (LSP) method could overcome the limitations associated with shot peening. Guo et al. (2019) tuned the surface morphology and compressive residual stresses by controlling the laser power density. The increase in surface roughness did not deteriorate the degradation rate due to the predominant effect of compressive residual stress. Rather, the grain refinement and compressive residual stress promoted the formation of a dense passive film and reduced the degradation rate by more than 45–52%. Ge et al. (2017) reported that two-sided LSP of AZ31B alloy reduced corrosion current and the stress corrosion cracking (SCC) susceptibility index by about 85 and 47%, respectively. The

TABLE 4 | Advantages and limitations of surface modification methods.

Surface modification method	Advantages	Limitations
Anodization	-Promote apatite formation -Improved degradation resistance -Improved biocompatibility	•Expensive •Deposition not hard enough •Non-uniform deposition •Cracks
Electrodeposition	-Favorable for apatite formation -Improved degradation resistance -Improved biocompatibility -PED has controlled porosity and degradation resistance	•Non-uniform porous coating •During prolonged immersion, the coating can be fragile •Substrate size and geometry
Electrophoretic deposition	-Uniform and dense coating -High purity deposition -Complex shapes are coated -Improved degradation resistance -Excellent biocompatibility and anti-bacterial property	•As-deposited EPD has poor adhesion •Process parameters need to be optimized
Plasma electrolytic oxidation	-Dense coating with porous outer layer -Promotes apatite formation -Suitable for pre-treatment -Improved degradation resistance -Excellent cytocompatibility and anti-bacterial property	•Corrosion medium penetrates through the porous structure •Less corrosion protection during prolonged immersion
Acid and alkali treatment	-Simple and cheap -Removes surface impurities -Increased surface energy -Excellent surface pre-treatment -Improved degradation resistance and bioactivity -Improves cytocompatibility	•Not suitable for prolonged durations •Poor coating quality
Hydrothermal treatment	-Cost-effective -Thin films with characteristic morphology -Suitable for pre-treatment -Improved degradation resistance -Improved biocompatibility and anti-bacterial property	•Not suitable for prolonged durations •Poor quality •Longer reaction time
Dip coating	-Low cost -Coat complex and large shapes -Excellent degradation resistance -Improved biocompatibility and anti-bacterial property	•Time-consuming •Non-uniform coating •Uncontrollable thickness
Spin coating	-Low coating time -Uniform coating -Less expensive -Excellent degradation resistance -Improved biocompatibility	•Limited coating area •Coating complex shapes •Difficult to create multi-layer coating
Electrospinning	-Relatively inexpensive -Coating morphology can be tuned similar to the extracellular matrix -Accelerated bioactivity -Excellent degradation resistance -Excellent biocompatibility and anti-bacterial property	•Sample size and geometry •Many process variables
Sputtering	-Better coating quality -Wide variety of materials can be deposited -Improved degradation resistance -Improved biocompatibility	•Expensive •Limited to thin coatings •Difficult to coat complex shapes
Thermal evaporation and ion plating	-High deposition rate -Relatively simple PVD process -Improved degradation resistance	•Relatively thin coatings •Cytocompatibility needs to be explored •Delamination during prolonged immersion
Chemical vapor deposition	-Controlled deposition with uniform thickness -Excellent for complex geometries -Excellent degradation resistance -Improved biocompatibility	•Delamination •Expensive •Limited substrate size
Thermal spray	-Wide range of coating materials	•High temperature affects coating materials' property

(Continued on following page)

TABLE 4 | (*Continued*) Advantages and limitations of surface modification methods.

Surface modification method	Advantages	Limitations
-Improved degradation resistance -Improved anti-bacterial resistance	-High deposition rates -Controlled coating morphology	•Difficult to achieve high coating thickness
Pulsed electron beam treatment	-Surface grain refinement -Removal of surface impurities -Enhance degradation resistance -Improved surface mechanical properties	•Crater defects •High surface roughness •Cytocompatibility needs to be explored
Laser surface treatment	-Characteristic dendritic and non-porous microstructure -Promotes apatite formation -Improved degradation resistance -Improved surface mechanical properties and wear resistance	•Thermal stress and crack formation •Expensive
SMAT and shot peening treatment	-High surface residual compressive stress -Improved surface mechanical properties and wear resistance	•Surface contamination •Poor degradation rate •No significant improvement for biocompatibility
LSP treatment	-High surface residual compressive stress -Better control over surface morphology -Improved surface mechanical properties and wear resistance	•Surface contamination •No significant improvement for degradation rate •No significant improvement for biocompatibility

improvement in degradation resistance was attributed to the fine grain refinement from 17.5 μm to 15.7 nm during LSP. A more significant number of grain boundaries acted as corrosion barriers by accelerating the passivation layer formation and reducing micro-galvanic couples between the interior of grains and grain boundaries. Zhang et al. (2018) also obtained improved mechanical properties and wear resistance without significantly improving degradation resistance and cytocompatibility. Xiong et al. (2020) investigated the effect of LSP, MAO, and LSP followed by MAO treatment on the stress corrosion cracking of AZ80 alloy in SBF. The favorable basal texture reconstructed along the (0002) plane during LSP/MAO treatment reduced E_{corr} by more than 300 mV and I_{corr} by more than two orders of magnitude.

Unlike conversion or deposition coating techniques, the surface metallurgical modifications techniques tailor the surface and subsurface microstructure. The disadvantages due to low coating adhesion and instability of the layer formed on the surface in the case of coating methods can be overcome by these techniques. The key findings from the surface metallurgical modification methods are included in **Table 3**.

SUMMARY

The emerging interest in developing biodegradable metallic implants for orthopedic applications has opened a new research direction to simultaneously tailoring the degradation and bioactivity of the Mg substrate through surface modification. As discussed in the previous sections, most reported methods demonstrated promising results for the intended application. However, constructing a stable surface on Mg substrate for a longer duration remains a challenge. The advantages and limitations of the possible surface modification methods discussed are summarized in **Table 4**.

The stability and adhesion of coatings on the substrate are a primary concern for implant applications. While the conversion methods provide better adhesion, their stability over a prolonged duration is yet to be ensured. Among the different conversion techniques discussed above, the EPD has shown the best performance in terms of stability and adhesion. Other conversion coatings like acid, alkali, and hydrothermal treatments have performed as excellent pre-treatment methods. The physical deposition methods help in providing stable scaffolds for improving bioactivity on the implant surfaces. However, their adhesion on the substrate needs to be enhanced for proper control of the degradation rate. It is suggested that a hybrid approach wherein the surface pre-treatment followed a proper physical deposition technique will help in tailoring the degradation and improving the bioactivity. Among surface metallurgical modifications, the uniform cellular microstructure exhibited by LSM had a significant effect on biodegradation behavior. Other methods significantly improved surface mechanical properties, but a drop in degradation resistance was observed due to surface contamination during processing. To summarize, the combination of different surface modification methods always exhibited remarkable improvement in degradation resistance, biocompatibility, and surface mechanical properties.

CONCLUSION AND FUTURE OUTLOOK

Mg being an exceptional biodegradable metal with its density and mechanical properties similar to those of human bone, there is a strong need to conduct further investigations to successfully implement Mg-based materials for temporary implants. The mechanism of major surface modification methods to optimize the degradation behavior and bioactivity of Mg with the recent research progresses in each method were discussed. It was understood that during *in vitro* tests, surface modification

seems to play a significant role in optimizing the biodegradation behavior of Mg-based materials during the initial stages.

The current review has discussed only the recent approaches for surface modification of biodegradable Mg-based alloys. However, the application of biologically active coatings and other surface technologies can be synergistically utilized to improve anti-bacterial properties as well. Moreover, the metallurgical modification needs to be considered to ensure the clinical outcome of Mg-based alloys for orthopedic applications. Additive manufacturing is another area of potential interest that has paved the way to precisely make medical implants even with complicated shapes. Looking at the future of orthopedic implants, developing and modifying the existing methods with broad characterization from a clinical perspective is suggested. The characterization should include surface morphology, mechanical properties, *in vitro* and *in vivo* degradation behavior, and, finally, the biocompatibility of the updated Mg-based alloy. A combination of mechanical processing and surface modification would be a promising design strategy to obtain an ideal Mg-based implant for temporary orthopedic applications. Furthermore, the development of a successful Mg-based alloy can be widened for permanent orthopedic fixations.

AUTHOR CONTRIBUTIONS

SR organized the data and drafted and revised the manuscript to the final version. MJ, TS, and HT contributed to the sections and critically revised the manuscript. All authors contributed to the manuscript revision and read and approved the submitted revision.

REFERENCES

Abdal-Hay, A., Dewidar, M., and Lim, J. K. (2012). Biocorrosion Behavior and Cell Viability of Adhesive Polymer Coated Magnesium Based Alloys for Medical Implants. *Appl. Surf. Sci.* 261, 536–546. doi:10.1016/j.apsusc.2012.08.051

Acheson, J. G., McKillop, S., Ward, J., Roy, A., Xu, Z., Boyd, A. R., et al. (2021). Effects of Strontium-Substitution in Sputter Deposited Calcium Phosphate Coatings on the Rate of Corrosion of Magnesium Alloys. *Surf. Coat. Tech.* 421, 127446. doi:10.1016/j.surfcoat.2021.127446

Aktug, S. L., Durdu, S., Aktas, S., Yalcin, E., and Usta, M. (2019). Surface and *In Vitro* Properties of Ag-Deposited Antibacterial and Bioactive Coatings on AZ31 Mg alloy. *Surf. Coat. Tech.* 375, 46–53. doi:10.1016/j.surfcoat.2019.07.013

Alaei, M., Atapour, M., and Labbaf, S. (2020). Electrophoretic Deposition of Chitosan-Bioactive Glass Nanocomposite Coatings on AZ91 Mg alloy for Biomedical Applications. *Prog. Org. Coat.* 147, 105803. doi:10.1016/j.porgcoat.2020.105803

Ali, A., Ikram, F., Iqbal, F., Fatima, H., Mehmood, A., Kolawole, M. Y., et al. (2021). Improving the *In Vitro* Degradation, Mechanical and Biological Properties of AZ91-3Ca Mg Alloy via Hydrothermal Calcium Phosphate Coatings. *Front. Mater.* 8. doi:10.3389/fmats.2021.715104

Askarnia, R., Fardi, S. R., Sobhani, M., and Staji, H. (2021). Ternary Hydroxyapatite/chitosan/graphene Oxide Composite Coating on AZ91D Magnesium alloy by Electrophoretic Deposition. *Ceramics Int.* 47, 27071–27081. doi:10.1016/j.ceramint.2021.06.120

Ba, Z., Dong, Q., Zhang, X., Wang, J., Yuan, C., and Liao, Y. (2016). Properties of Zr2ON2 Film Deposited on Mg-Gd-Zn alloy with Mg-Al Hydrotalcite Film by Arc Ion Plating. *Surf. Coat. Tech.* 294, 67–74. doi:10.1016/j.surfcoat.2016.03.073

Bagherifard, S., Hickey, D. J., Fintová, S., Pastorek, F., Fernandez-Pariente, I., Bandini, M., et al. (2018). Effects of Nanofeatures Induced by Severe Shot Peening (SSP) on Mechanical, Corrosion and Cytocompatibility Properties of Magnesium alloy AZ31. *Acta Biomater.* 66, 93–108. doi:10.1016/j.actbio.2017.11.032

Bakhsheshi-Rad, H. R., Ismail, A. F., Aziz, M., Akbari, M., Hadisi, Z., Khoshnava, S. M., et al. (2020). Co-incorporation of Graphene Oxide/silver Nanoparticle into Poly-L-Lactic Acid Fibrous: A Route toward the Development of Cytocompatible and Antibacterial Coating Layer on Magnesium Implants. *Mater. Sci. Eng. C* 111, 110812. doi:10.1016/j.msec.2020.110812

Bakhsheshi-Rad, H. R., Ismail, A. F., Aziz, M., Hadisi, Z., Omidi, M., and Chen, X. (2019). Antibacterial Activity and Corrosion Resistance of Ta2O5 Thin Film and Electrospun PCL/MgO-Ag Nanofiber Coatings on Biodegradable Mg alloy Implants. *Ceramics Int.* 45, 11883–11892. doi:10.1016/j.ceramint.2019.03.071

Bansal, P., Singh, G., and Sidhu, H. S. (2020). Investigation of Surface Properties and Corrosion Behavior of Plasma Sprayed HA/ZnO Coatings Prepared on AZ31 Mg alloy. *Surf. Coat. Tech.* 401, 126241. doi:10.1016/j.surfcoat.2020.126241

Bansal, P., Singh, G., and Sidhu, H. S. (2021). Plasma-Sprayed Hydroxyapatite-Strontium Coating for Improved Corrosion Resistance and Surface Properties of Biodegradable AZ31 Mg Alloy for Biomedical Applications. *J. Materi Eng. Perform.* 30, 1768–1779. doi:10.1007/s11665-021-05490-0

Bryła, K., Horky, J., Krystian, M., Lityńska-Dobrzyńska, L., and Mingler, B. (2020). Microstructure, Mechanical Properties, and Degradation of Mg-Ag alloy after Equal-Channel Angular Pressing. *Mater. Sci. Eng. C* 109, 110543. doi:10.1016/j.msec.2019.110543

Calderón, D., Galindez, Y., Toro, L., Zuleta, A. A., Valencia-Escobar, A., Chacón, P., et al. (2021). Intermetallic-Rich Layer Formation for Improving Corrosion Resistance of Magnesium Alloys. *Met. Mater. Int*. doi:10.1007/s12540-020-00912-5

Chandra, G., and Pandey, A. (2021). Design Approaches and Challenges for Biodegradable Bone Implants: a Review. *Expert Rev. Med. Devices* 18, 1–19. doi:10.1080/17434440.2021.1935875

Chen, G., Fu, Y., Cui, Y., Gao, J., Guo, X., Gao, H., et al. (2019a). Effect of Surface Mechanical Attrition Treatment on Corrosion Fatigue Behavior of AZ31B Magnesium alloy. *Int. J. Fatigue* 127, 461–469. doi:10.1016/j.ijfatigue.2019.06.031

Chen, H., Kang, F., Luo, Z., and Liu, J. (2019b). MgF 2/MgO Composite Coating on Porous Magnesium Surface and its Biocorrosion Resistance. *Mater. Corrosion* 70, 1242–1251. doi:10.1002/maco.201810456

Chen, X.-B., Chong, K., Abbott, T. B., Birbilis, N., and Easton, M. A. (2015). "Biocompatible Strontium-Phosphate and Manganese-Phosphate Conversion Coatings for Magnesium and its Alloys" in *Surface Modification Of Magnesium And its Alloys For Biomedical Applications*. Cambridge, United Kingdom: Woodhead Publishing, 407–432. doi:10.1016/B978-1-78242-078-1.00015-3

Cheng, S., Lan, L., Li, M., Chu, X., Zhong, H., Yao, M., et al. (2021). Pure Mg-Al Layered Double Hydroxide Film on Magnesium Alloys for Orthopedic Applications. *ACS Omega* 6, 24575–24584. doi:10.1021/acsomega.1c03169

Chopra, D., Gulati, K., and Ivanovski, S. (2021). Bed of Nails: Bioinspired Nano-Texturing towards Antibacterial and Bioactivity Functions. *Mater. Today Adv.* 12, 100176. doi:10.1016/j.mtadv.2021.100176

Cipriano, A. F., Lin, J., Miller, C., Lin, A., Cortez Alcaraz, M. C., Soria, P., et al. (2017). Anodization of Magnesium for Biomedical Applications - Processing, Characterization, Degradation and Cytocompatibility. *Acta Biomater.* 62, 397–417. doi:10.1016/j.actbio.2017.08.017

Daroonparvar, M., Farooq Khan, M. U., Saadeh, Y., Kay, C. M., Gupta, R. K., Kasar, A. K., et al. (2020). Enhanced Corrosion Resistance and Surface Bioactivity of AZ31B Mg alloy by High Pressure Cold Sprayed Monolayer Ti and Bilayer Ta/Ti Coatings in Simulated Body Fluid. *Mater. Chem. Phys.* 256, 123627. doi:10.1016/j.matchemphys.2020.123627

Daroonparvar, M., Mat Yajid, M. A., Kumar Gupta, R., Mohd Yusof, N., Bakhsheshi-Rad, H. R., Ghandvar, H., et al. (2018). Antibacterial Activities and Corrosion Behavior of Novel PEO/nanostructured ZrO2 Coating on Mg alloy. *Trans. Nonferrous Met. Soc. China* 28, 1571–1581. doi:10.1016/S1003-6326(18)64799-5

Dauwe, J., Walters, G., Holzer, L. A., Vanhaecht, K., and Nijs, S. (2020). Failure after Proximal Humeral Fracture Osteosynthesis: a One Year Analysis of Hospital-Related Healthcare Cost. *Int. Orthopaedics (Sicot)* 44, 1217–1221. doi:10.1007/s00264-020-04577-y

de Oliveira, L. A., da Silva, R. M. P., Rodas, A. C. D., Souto, R. M., and Antunes, R. A. (2020). Surface Chemistry, Film Morphology, Local Electrochemical Behavior and Cytotoxic Response of Anodized AZ31B Magnesium alloy. *J. Mater. Res. Tech.* 9, 14754–14770. doi:10.1016/j.jmrt.2020.10.063

Fernández-Hernán, J. P., Torres, B., López, A. J., Martínez-Campos, E., and Rams, J. (2021). Sol-gel Coatings Doped with Graphene Nanoplatelets for Improving the Degradation Rate and the Cytocompatibility of AZ31 alloy for Biomedical Applications. *Surf. Coat. Tech.* 426, 127745. doi:10.1016/j.surfcoat.2021.127745

Figueira, R. B. (2020). Hybrid Sol-Gel Coatings for Corrosion Mitigation: A Critical Review. *Polymers* 12, 689. doi:10.3390/polym12030689

Fong, J. S. L., Booth, M. A., Rifai, A., Fox, K., and Gelmi, A. (2021). Diamond in the Rough: Toward Improved Materials for the Bone–Implant Interface. *Adv. Healthc. Mater.* 10, 2100007. doi:10.1002/adhm.202100007

Gao, B., Hao, S., Zou, J., Wu, W., Tu, G., and Dong, C. (2007). Effect of High Current Pulsed Electron Beam Treatment on Surface Microstructure and Wear and Corrosion Resistance of an AZ91HP Magnesium alloy. *Surf. Coat. Tech.* 201, 6297–6303. doi:10.1016/j.surfcoat.2006.11.036

Gawlik, M. M., Wiese, B., Welle, A., González, J., Desharnais, V., Harmuth, J., et al. (2019). Acetic Acid Etching of Mg-xGd Alloys. *Metals* 9, 117–119. doi:10.3390/met9020117

Ge, M.-Z., Xiang, J.-Y., Yang, L., and Wang, J. T. (2017). Effect of Laser Shock Peening on the Stress Corrosion Cracking of AZ31B Magnesium alloy in a Simulated Body Fluid. *Surf. Coat. Tech.* 310, 157–165. doi:10.1016/j.surfcoat.2016.12.093

Ghafarzadeh, M., Kharaziha, M., and Atapour, M. (2021). Bilayer Micro-arc Oxidation-Poly (Glycerol Sebacate) Coating on AZ91 for Improved Corrosion Resistance and Biological Activity. *Prog. Org. Coat.* 161, 106495. doi:10.1016/j.porgcoat.2021.106495

Gowri, S., Rajiv Gandhi, R., and Sundrarajan, M. (2014). Structural, Optical, Antibacterial and Antifungal Properties of Zirconia Nanoparticles by Biobased Protocol. *J. Mater. Sci. Tech.* 30, 782–790. doi:10.1016/j.jmst.2014.03.002

Grzeskowiak, R. M., Schumacher, J., Dhar, M. S., Harper, D. P., Mulon, P.-Y., and Anderson, D. E. (2020). Bone and Cartilage Interfaces with Orthopedic Implants: A Literature Review. *Front. Surg.* 7. doi:10.3389/fsurg.2020.601244

Gu, X. N., Zheng, W., Cheng, Y., and Zheng, Y. F. (2009). A Study on Alkaline Heat Treated Mg-Ca alloy for the Control of the Biocorrosion Rate. *Acta Biomater.* 5, 2790–2799. doi:10.1016/j.actbio.2009.01.048

Guan, Y. C., Zhou, W., and Zheng, H. Y. (2009). Effect of Laser Surface Melting on Corrosion Behaviour of AZ91D Mg alloy in Simulated-Modified Body Fluid. *J. Appl. Electrochem.* 39, 1457–1464. doi:10.1007/s10800-009-9825-2

Guo, C., Wang, L., Zhou, J., Cao, B., Xu, Y., Almaqrami, B. S., et al. (2021). Effect of Grain Refinement by Laser Surface Treatment on Cell Adhesion Behavior of AZ91D Magnesium Alloy. *J. Test. Eval.* 49, 20180779–20181715. doi:10.1520/JTE20180779

Guo, H. F., An, M. Z., Huo, H. B., Xu, S., and Wu, L. J. (2006). Microstructure Characteristic of Ceramic Coatings Fabricated on Magnesium Alloys by Micro-arc Oxidation in Alkaline Silicate Solutions. *Appl. Surf. Sci.* 252, 7911–7916. doi:10.1016/j.apsusc.2005.09.067

Guo, Y., Su, Y., Gu, R., Zhang, Z., Li, G., Lian, J., et al. (2020). Enhanced Corrosion Resistance and Biocompatibility of Biodegradable Magnesium alloy Modified by Calcium Phosphate/collagen Coating. *Surf. Coat. Tech.* 401, 126318. doi:10.1016/j.surfcoat.2020.126318

Guo, Y., Wang, S., Liu, W., Xiao, T., Zhu, G., and Sun, Z. (2019). The Effect of Laser Shock Peening on the Corrosion Behavior of Biocompatible Magnesium Alloy ZK60. *Metals* 9, 1237. doi:10.3390/met9111237

Hamghavandi, M. R., Montazeri, A., Ahmadi Daryakenari, A., and Pishvaei, M. (2021). Preparation and Characterization of Chitosan/graphene Oxide Nanocomposite Coatings on Mg-2 Wt% Zn Scaffold by Pulse Electrodeposition Process. *Biomed. Mater.* 16, 065005. doi:10.1088/1748-605X/ac1f9f

Hanas, T., Sampath Kumar, T. S., Perumal, G., and Doble, M. (2016). Tailoring Degradation of AZ31 alloy by Surface Pre-treatment and Electrospun PCL Fibrous Coating. *Mater. Sci. Eng. C* 65, 43–50. doi:10.1016/j.msec.2016.04.017

Heimann, R. B. (2021). Magnesium Alloys for Biomedical Application: Advanced Corrosion Control through Surface Coating. *Surf. Coat. Tech.* 405, 126521. doi:10.1016/j.surfcoat.2020.126521

Herteleer, M., De Jaegere, A., Winckelmans, T., Casteur, H., Nijs, S., and Hoekstra, H. (2021). Healthcare Utilization and Related Cost of Midshaft Clavicle Fracture Treatment in Belgium. *Eur. J. Trauma Emerg. Surg.* 47, 1281–1287. doi:10.1007/s00068-020-01307-2

Hou, S., Yu, W., Yang, Z., Li, Y., Yang, L., and Lang, S. (2020). Properties of Titanium Oxide Coating on MgZn Alloy by Magnetron Sputtering for Stent Application. *Coatings* 10, 999. doi:10.3390/coatings10100999

Hughes, A. E. (2018). *"Conversion Coatings," in* Encyclopedia Of Interfacial Chemistry: Surface Science And Electrochemistry. Elsevier, 108–114. doi:10.1016/B978-0-12-409547-2.13441-9Conversion Coatings.

Jacob, G., Shimomura, K., and Nakamura, N. (2020). Osteochondral Injury, Management and Tissue Engineering Approaches. *Front. Cel Dev. Biol.* 8, 580868. doi:10.3389/fcell.2020.580868

Jahr, H., Li, Y., Zhou, J., Zadpoor, A. A., and Schröder, K.-U. (2021). Additively Manufactured Absorbable Porous Metal Implants - Processing, Alloying and Corrosion Behavior. *Front. Mater.* 8. doi:10.3389/fmats.2021.628633

Jiang, S., Cai, S., Lin, Y., Bao, X., Ling, R., Xie, D., et al. (2019). Effect of Alkali/acid Pretreatment on the Topography and Corrosion Resistance of As-Deposited CaP Coating on Magnesium Alloys. *J. Alloys Comp.* 793, 202–211. doi:10.1016/j.jallcom.2019.04.198

Jiao, J., Zhang, S., Qu, X., and Yue, B. (2021). Recent Advances in Research on Antibacterial Metals and Alloys as Implant Materials. *Front. Cel. Infect. Microbiol.* 11. doi:10.3389/fcimb.2021.693939

Kania, A., Pilarczyk, W., and Szindler, M. M. (2020). Structure and Corrosion Behavior of TiO2 Thin Films Deposited onto Mg-Based alloy Using Magnetron Sputtering and Sol-Gel. *Thin Solid Films* 701, 137945. doi:10.1016/j.tsf.2020.137945

Karthega, M., Pranesh, M., Poongothai, C., and Srinivasan, N. (2021). Poly Caprolactone/titanium Dioxide Nanofiber Coating on AM50 alloy for Biomedical Application. *J. Magnesium Alloys* 9, 532–547. doi:10.1016/j.jma.2020.07.003

Khan, M., Osman, K., Green, G., and Haddad, F. S. (2016). The Epidemiology of Failure in Total Knee Arthroplasty. *Bone Jt. J.* 98-B, 105–112. doi:10.1302/0301-620x.98b1.36293

Kim, S.-M., Kang, M.-H., Kim, H.-E., Lim, H.-K., Byun, S.-H., Lee, J.-H., et al. (2017). Innovative Micro-textured Hydroxyapatite and poly(L-Lactic)-Acid Polymer Composite Film as a Flexible, Corrosion Resistant, Biocompatible, and Bioactive Coating for Mg Implants. *Mater. Sci. Eng. C* 81, 97–103. doi:10.1016/j.msec.2017.07.026

Kirkland, N. T., and Birbilis, N. (2014). *Magnesium Biomaterials: Design, Testing, and Best Practice*. Springer International Publishing, 1–12. doi:10.1007/978-3-319-02123-2_1Introduction to Magnesium Biomaterials.

Kozina, I., Krawiec, H., Starowicz, M., and Kawalec, M. (2021). Corrosion Resistance of MgZn Alloy Covered by Chitosan-Based Coatings. *Ijms* 22, 8301. doi:10.3390/ijms22158301

Laleh, M., and Kargar, F. (2011). Effect of Surface Nanocrystallization on the Microstructural and Corrosion Characteristics of AZ91D Magnesium alloy. *J. Alloys Comp.* 509, 9150–9156. doi:10.1016/j.jallcom.2011.06.094

Lee, D., Kim, B., Baek, S.-M., Kim, J., Park, H. W., Lee, J. G., et al. (2020). Microstructure and Corrosion Resistance of a Mg2Sn-Dispersed Mg alloy Subjected to Pulsed Electron Beam Treatment. *J. Magnesium Alloys* 8, 345–351. doi:10.1016/j.jma.2020.02.005

Lee, W. J., Kim, J., and Park, H. W. (2019). Improved Corrosion Resistance of Mg alloy AZ31B Induced by Selective Evaporation of Mg Using Large Pulsed Electron Beam Irradiation. *J. Mater. Sci. Tech.* 35, 891–901. doi:10.1016/j.jmst.2018.12.004

Li, C., Guo, C., Fitzpatrick, V., Ibrahim, A., Zwierstra, M. J., Hanna, P., et al. (2020a). Design of Biodegradable, Implantable Devices towards Clinical Translation. *Nat. Rev. Mater.* 5, 61–81. doi:10.1038/s41578-019-0150-z

Li, N., Li, Y. D., Li, Y. X., Wu, Y. H., Zheng, Y. F., and Han, Y. (2014). Effect of Surface Mechanical Attrition Treatment on Biodegradable Mg-1Ca alloy. *Mater. Sci. Eng. C* 35, 314–321. doi:10.1016/j.msec.2013.11.010

Li, Q., Bao, X., Sun, J. e., Cai, S., Xie, Y., Liu, Y., et al. (2021a). Fabrication of Superhydrophobic Composite Coating of Hydroxyapatite/stearic Acid on

Magnesium alloy and its Corrosion Resistance, Antibacterial Adhesion. *J. Mater. Sci.* 56, 5233–5249. doi:10.1007/s10853-020-05592-5

Li, S., Yi, L., Liu, T., Deng, H., Ji, B., Zhang, K., et al. (2020b). Formation of a Protective Layer against Corrosion on Mg alloy via Alkali Pretreatment Followed by Vanillic Acid Treatment. *Mater. Corrosion* 71, 1330–1338. doi:10.1002/maco.201911488

Li, W., Qiao, W., Liu, X., Bian, D., Shen, D., Zheng, Y., et al. (2021b). Biomimicking Bone-Implant Interface Facilitates the Bioadaption of a New Degradable Magnesium Alloy to the Bone Tissue Microenvironment. *Adv. Sci.* 8, 1–7. doi:10.1002/advs.202102035

Liang, D.-y., Liang, P.-c., Yi, Q.-q., Sha, S., Shi, J.-f., and Chang, Q. (2021). Copper Coating Formed by Micro-arc Oxidation on Pure Mg Improved Antibacterial Activity, Osteogenesis, and Angiogenesis *In Vivo* and *In Vitro*. *Biomed. Microdevices* 23. doi:10.1007/s10544-021-00573-0

Liu, J., Fang, X., Zhu, C., Xing, X., Cui, G., and Li, Z. (2020). Fabrication of Superhydrophobic Coatings for Corrosion protection by Electrodeposition: A Comprehensive Review. *Colloids Surf. A: Physicochemical Eng. Aspects* 607, 125498. doi:10.1016/j.colsurfa.2020.125498

Liu, L., Yang, Q., Huang, L., Liu, X., Liang, Y., Cui, Z., et al. (2019). The Effects of a Phytic Acid/calcium Ion Conversion Coating on the Corrosion Behavior and Osteoinductivity of a Magnesium-Strontium alloy. *Appl. Surf. Sci.* 484, 511–523. doi:10.1016/j.apsusc.2019.04.107

Liu, Y., Cheng, X., Wang, X., Sun, Q., Wang, C., Di, P., et al. (2021). Micro-arc Oxidation-Assisted Sol-Gel Preparation of Calcium Metaphosphate Coatings on Magnesium Alloys for Bone Repair. *Mater. Sci. Eng. C* 131, 112491. doi:10.1016/j.msec.2021.112491

L., M., Kar, S., B., N., Dhilip Kumar, S. S., Nagai, M., and Santra, T. S. (2020). Formation of Nanostructures on Magnesium alloy by Anodization for Potential Biomedical Applications. *Mater. Today Commun.* 25, 101403. doi:10.1016/j.mtcomm.2020.101403

Lu, J. Z., Joshi, S. S., Pantawane, M. V., Ho, Y.-H., Wu, T.-C., and Dahotre, N. B. (2019). Optimization of Biocompatibility in a Laser Surface Treated Mg-AZ31B alloy. *Mater. Sci. Eng. C* 105, 110028. doi:10.1016/j.msec.2019.110028

Luan, B. L., Yang, D., Liu, X. Y., and Song, G.-L. (2011). "Corrosion protection of Magnesium (Mg) Alloys Using Conversion and Electrophoretic Coatings" in *Corrosion of Magnesium Alloys*. Cambridge, United Kingdom: Woodhead Publishing, 541–564. doi:10.1533/9780857091413.4.541

Luo, Y., Zhang, C., Wang, J., Liu, F., Chau, K. W., Qin, L., et al. (2021). Clinical Translation and Challenges of Biodegradable Magnesium-Based Interference Screws in ACL Reconstruction. *Bioactive Mater.* 6, 3231–3243. doi:10.1016/j.bioactmat.2021.02.032

Manne, B., Thiruvayapati, H., Bontha, S., Motagondanahalli Rangarasaiah, R., Das, M., and Balla, V. K. (2018). Surface Design of Mg-Zn alloy Temporary Orthopaedic Implants: Tailoring Wettability and Biodegradability Using Laser Surface Melting. *Surf. Coat. Tech.* 347, 337–349. doi:10.1016/j.surfcoat.2018.05.017

Mao, L., Yuan, G., Niu, J., Zong, Y., and Ding, W. (2013). *In Vitro* degradation Behavior and Biocompatibility of Mg-Nd-Zn-Zr alloy by Hydrofluoric Acid Treatment. *Mater. Sci. Eng. C* 33, 242–250. doi:10.1016/j.msec.2012.08.036

Mardali, M., SalimiJazi, H. R., Karimzadeh, F., Luthringer, B., Blawert, C., and Labbaf, S. (2019). Comparative Study on Microstructure and Corrosion Behavior of Nanostructured Hydroxyapatite Coatings Deposited by High Velocity Oxygen Fuel and Flame Spraying on AZ61 Magnesium Based Substrates. *Appl. Surf. Sci.* 465, 614–624. doi:10.1016/j.apsusc.2018.09.127

Mhaede, M., Pastorek, F., and Hadzima, B. (2014). Influence of Shot Peening on Corrosion Properties of Biocompatible Magnesium alloy AZ31 Coated by Dicalcium Phosphate Dihydrate (DCPD). *Mater. Sci. Eng. C* 39, 330–335. doi:10.1016/j.msec.2014.03.023

Morini, F., Bestetti, M., Franz, S., Vicenzo, A., Markov, A., and Yakovlev, E. (2021). Surface Properties Modification of Magnesium Alloys by Low Energy High Current Pulsed Electron Beam. *Surf. Coat. Tech.* 420, 127351. doi:10.1016/j.surfcoat.2021.127351

Mousa, H. M., Mahmoud, M. A., Yasin, A. S., and Mohamed, I. M. A. (2021). Polycaprolactone Tridentate Ligand Corrosion Inhibitors Coated on Biodegradable Mg Implant. *J. Coat. Technol. Res.* 18, 1191–1197. doi:10.1007/s11998-021-00478-w

Muñoz, M., Torres, B., Mohedano, M., Matykina, E., Arrabal, R., López, A. J., et al. (2020). PLA Deposition on Surface Treated Magnesium alloy: Adhesion, Toughness and Corrosion Behaviour. *Surf. Coat. Tech.* 388, 125593. doi:10.1016/j.surfcoat.2020.125593

Nikbakht, A., Dehghanian, C., and Parichehr, R. (2021). Silane Coatings Modified with Hydroxyapatite Nanoparticles to Enhance the Biocompatibility and Corrosion Resistance of a Magnesium alloy. *RSC Adv.* 11, 26127–26144. doi:10.1039/d1ra01018b

Nwaogu, U. C., Blawert, C., Scharnagl, N., Dietzel, W., and Kainer, K. U. (2010). Effects of Organic Acid Pickling on the Corrosion Resistance of Magnesium alloy AZ31 Sheet. *Corrosion Sci.* 52, 2143–2154. doi:10.1016/j.corsci.2010.03.002

Omar, S. A., Ballarre, J., Castro, Y., Martinez Campos, E., Schreiner, W., Durán, A., et al. (2020). 58S and 68S Sol-Gel Glass-like Bioactive Coatings for Enhancing the Implant Performance of AZ91D Magnesium alloy. *Surf. Coat. Tech.* 400, 126224. doi:10.1016/j.surfcoat.2020.126224

Panahi, Z., Tamjid, E., and Rezaei, M. (2020). Surface Modification of Biodegradable AZ91 Magnesium alloy by Electrospun Polymer Nanocomposite: Evaluation of *In Vitro* Degradation and Cytocompatibility. *Surf. Coat. Tech.* 386, 125461. doi:10.1016/j.surfcoat.2020.125461

Peral, L. B., Zafra, A., Bagherifard, S., Guagliano, M., and Fernández-Pariente, I. (2020). Effect of Warm Shot Peening Treatments on Surface Properties and Corrosion Behavior of AZ31 Magnesium alloy. *Surf. Coat. Tech.* 401, 126285. doi:10.1016/j.surfcoat.2020.126285

Peron, M., Bertolini, R., and Cogo, S. (2022). On the Corrosion, Stress Corrosion and Cytocompatibility Performances of ALD TiO2 and ZrO2 Coated Magnesium Alloys. *J. Mech. Behav. Biomed. Mater.* 125, 104945. doi:10.1016/j.jmbbm.2021.104945

Peron, M., Bin Afif, A., Dadlani, A. L., Berto, F., and Torgersen, J. (2020). Improving Stress Corrosion Cracking Behavior of AZ31 alloy with Conformal Thin Titania and Zirconia Coatings for Biomedical Applications. *J. Mech. Behav. Biomed. Mater.* 111, 104005. doi:10.1016/j.jmbbm.2020.104005

Perumal, G., Ramasamy, B., Nandkumar A, M., Dhanasekaran, S., Ramasamy, S., and Doble, M. (2020). Bilayer Nanostructure Coated AZ31 Magnesium alloy Implants: *In Vivo* Reconstruction of Critical-Sized Rabbit Femoral Segmental Bone Defect. *Nanomedicine: Nanotechnology, Biol. Med.* 29, 102232. doi:10.1016/j.nano.2020.102232

Qin, Y., Wen, P., Guo, H., Xia, D., Zheng, Y., Jauer, L., et al. (2019). Additive Manufacturing of Biodegradable Metals: Current Research Status and Future Perspectives. *Acta Biomater.* 98, 3–22. doi:10.1016/j.actbio.2019.04.046

Rahim, S. A., Joseph, M. A., and T, H. (2020). Tailoring Biomineralization and Biodegradation of Mg-Ca alloy by Acetic Acid Pickling. *Mater. Res. Express* 7, 054002. doi:10.1088/2053-1591/ab8d5f

Rahim, S. A., Muhammad Rabeeh, V., Joseph, M. A., and Hanas, T. (2021a). Does Acid Pickling of Mg-Ca alloy Enhance Biomineralization? *J. Magnesium Alloys* 9, 1028–1038. doi:10.1016/j.jma.2020.12.002

Rahim, S. A., Nikhil, T. T., Joseph, M. A., and Hanas, T. (2021b). *In Vitro* degradation and Mechanical Behaviour of Calcium Phosphate Coated Mg-Ca alloy. *Mater. Tech.* 36, 738–746. doi:10.1080/10667857.2020.1794278

Rahman, M., Dutta, N. K., and Roy Choudhury, N. (2020). Magnesium Alloys with Tunable Interfaces as Bone Implant Materials. *Front. Bioeng. Biotechnol.* 8. doi:10.3389/fbioe.2020.00564

Rahman, Z. U., Deen, K. M., and Haider, W. (2019). Controlling Corrosion Kinetics of Magnesium Alloys by Electrochemical Anodization and Investigation of Film Mechanical Properties. *Appl. Surf. Sci.* 484, 906–916. doi:10.1016/j.apsusc.2019.02.168

Rakesh, K. R., Bontha, S., M. R., R., Das, M., and Balla, V. K. (2019). Laser Surface Melting of Mg-Zn-Dy alloy for Better Wettability and Corrosion Resistance for Biodegradable Implant Applications. *Appl. Surf. Sci.* 480, 70–82. doi:10.1016/j.apsusc.2019.02.167

Rezk, A. I., Mousa, H. M., Lee, J., Park, C. H., and Kim, C. S. (2019). Composite PCL/HA/simvastatin Electrospun Nanofiber Coating on Biodegradable Mg alloy for Orthopedic Implant Application. *J. Coat. Technol. Res.* 16, 477–489. doi:10.1007/s11998-018-0126-8

Rojaee, R., Fathi, M., and Raeissi, K. (2013). Controlling the Degradation Rate of AZ91 Magnesium alloy via Sol-Gel Derived Nanostructured Hydroxyapatite Coating. *Mater. Sci. Eng. C* 33, 3817–3825. doi:10.1016/j.msec.2013.05.014

Saadati, A., Khiarak, B. N., Zahraei, A. A., Nourbakhsh, A., and Mohammadzadeh, H. (2021). Electrochemical Characterization of Electrophoretically Deposited

Hydroxyapatite/chitosan/graphene Oxide Composite Coating on Mg Substrate. *Surf. Inter.* 25, 101290. doi:10.1016/j.surfin.2021.101290

Saberi, A., Bakhsheshi-Rad, H. R., Abazari, S., Ismail, A. F., Sharif, S., Ramakrishna, S., et al. (2021). A Comprehensive Review on Surface Modifications of Biodegradable Magnesium-Based Implant alloy: Polymer Coatings Opportunities and Challenges. *Coatings* 11, 747. doi:10.3390/coatings11070747

Saxena, A., and Raman, R. K. S. (2021). Role of Surface Preparation in Corrosion Resistance Due to Silane Coatings on a Magnesium alloy. *Molecules* 26, 1–17. doi:10.3390/molecules26216663

Schumacher, S. A., Toribio, R. E., Lakritz, J., and Bertone, A. L. (2019). Radio-Telemetric Assessment of Cardiac Variables and Locomotion with Experimentally Induced Hypermagnesemia in Horses Using Chronically Implanted Catheters. *Front. Vet. Sci.* 6. doi:10.3389/fvets.2019.00414

Seyfi, M., Fattah-alhosseini, A., Pajohi-Alamoti, M., and Nikoomanzari, E. (2021). Effect of ZnO Nanoparticles Addition to PEO Coatings on AZ31B Mg alloy: Antibacterial Effect and Corrosion Behavior of Coatings in Ringer's Physiological Solution. *J. Asian Ceram. Societies* 9, 1114–1127. doi:10.1080/21870764.2021.1940728

Shang, Z., Li, D., Chen, J., Wang, M., Zhang, B., Wang, X., et al. (2021). The Role of Biodegradable Magnesium and its Alloys in Anterior Cruciate Ligament Reconstruction: A Systematic Review and Meta-Analysis Based on Animal Studies. *Front. Bioeng. Biotechnol.* 9. doi:10.3389/fbioe.2021.789498

Shi, H., Zhou, P., Li, J., Liu, C., and Wang, L. (2021). Functional Gradient Metallic Biomaterials: Techniques, Current Scenery, and Future Prospects in the Biomedical Field. *Front. Bioeng. Biotechnol.* 8. doi:10.3389/fbioe.2020.616845

Singh, B., Singh, G., Sidhu, B. S., and Bhatia, N. (2019). *In-vitro* Assessment of HA-Nb Coating on Mg alloy ZK60 for Biomedical Applications. *Mater. Chem. Phys.* 231, 138–149. doi:10.1016/j.matchemphys.2019.04.037

Singh, D., Basha, D. A., Wadsö, L., Orlov, D., Matsushita, Y., Singh, A., et al. (2021a). Evolution of Gradient Structured Layer on AZ91D Magnesium alloy and its Corrosion Behaviour. *J. Alloys Comp.* 882, 160659. doi:10.1016/j.jallcom.2021.160659

Singh, N., Batra, U., Kumar, K., and Mahapatro, A. (2021b). Investigating TiO2-HA-PCL Hybrid Coating as an Efficient Corrosion Resistant Barrier of ZM21 Mg alloy. *J. Magnesium Alloys* 9, 627–646. doi:10.1016/j.jma.2020.08.003

Skowron, K., Dryzek, E., Wróbel, M., Nowak, P., Marciszko-Wiąckowska, M., Le Joncour, L., et al. (2020). Gradient Microstructure Induced by Surface Mechanical Attrition Treatment (SMAT) in Magnesium Studied Using Positron Annihilation Spectroscopy and Complementary Methods. *Materials* 13, 4002–4024. doi:10.3390/ma13184002

Song, Y., Zhang, S., Li, J., Zhao, C., and Zhang, X. (2010). Electrodeposition of Ca-P Coatings on Biodegradable Mg alloy: *In Vitro* Biomineralization Behavior☆. *Acta Biomater.* 6, 1736–1742. doi:10.1016/j.actbio.2009.12.020

Su, Y., Lu, C., Hu, X., Guo, Y., Xun, X., Zhang, Z., et al. (2018). Improving the Degradation Resistance and Surface Biomineralization Ability of Calcium Phosphate Coatings on a Biodegradable Magnesium Alloy via a Sol-Gel Spin Coating Method. *J. Electrochem. Soc.* 165, C155–C161. doi:10.1149/2.0901803jes

Surmeneva, M. A., Ivanova, A. A., Tian, Q., Pittman, R., Jiang, W., Lin, J., et al. (2019). Bone Marrow Derived Mesenchymal Stem Cell Response to the RF Magnetron Sputter Deposited Hydroxyapatite Coating on AZ91 Magnesium alloy. *Mater. Chem. Phys.* 221, 89–98. doi:10.1016/j.matchemphys.2018.09.030

Surmeneva, M. A., Mukhametkaliyev, T. M., Khakbaz, H., Surmenev, R. A., and Bobby Kannan, M. (2015). Ultrathin Film Coating of Hydroxyapatite (HA) on a Magnesium-Calcium alloy Using RF Magnetron Sputtering for Bioimplant Applications. *Mater. Lett.* 152, 280–282. doi:10.1016/j.matlet.2015.03.140

T, D. T., Rahim, S. A., and T, H. (2019). Polyvinyl Alcohol/magnesium Phosphate Composite Coated Mg-Ca alloy for Biodegradable Orthopaedic Implant Applications. *Mater. Res. Express* 6, 1165b7. doi:10.1088/2053-1591/ab4d83

T, H., Sampath Kumar, T. S., Perumal, G., Doble, M., and Ramakrishna, S. (2018). Electrospun PCL/HA Coated Friction Stir Processed AZ31/HA Composites for Degradable Implant Applications. *J. Mater. Process. Tech.* 252, 398–406. doi:10.1016/j.jmatprotec.2017.10.009

Tang, H., Wu, T., Xu, F., Tao, W., and Jian, X. (2017). Fabrication and Characterization of Mg(OH)2 Films on AZ31 Magnesium Alloy by Alkali Treatment. *Int. J. Electrochem. Sci.* 12, 1377–1388. doi:10.20964/2017.02.35

Uddin, M., Hall, C., and Santos, V. (2020). Fabrication, Characterisation and Corrosion of HA Coated AZ31B Mg Implant Material: Effect of Electrodeposition Current Density. *Surf. Coat. Tech.* 385, 125363. doi:10.1016/j.surfcoat.2020.125363

Wang, C., Fang, H., Hang, C., Sun, Y., Peng, Z., Wei, W., et al. (2020a). Fabrication and Characterization of Silk Fibroin Coating on APTES Pretreated Mg-Zn-Ca alloy. *Mater. Sci. Eng. C* 110, 110742. doi:10.1016/j.msec.2020.110742

Wang, C., Yi, Z., Sheng, Y., Tian, L., Qin, L., Ngai, T., et al. (2019a). Development of a Novel Biodegradable and Anti-bacterial Polyurethane Coating for Biomedical Magnesium Rods. *Mater. Sci. Eng. C* 99, 344–356. doi:10.1016/j.msec.2019.01.119

Wang, H. X., Guan, S. K., Wang, X., Ren, C. X., and Wang, L. G. (2010). *In Vitro* degradation and Mechanical Integrity of Mg-Zn-Ca alloy Coated with Ca-Deficient Hydroxyapatite by the Pulse Electrodeposition Process☆. *Acta Biomater.* 6, 1743–1748. doi:10.1016/j.actbio.2009.12.009

Wang, J. L., Xu, J. K., Hopkins, C., Chow, D. H. K., and Qin, L. (2020b). Biodegradable Magnesium-Based Implants in Orthopedics-A General Review and Perspectives. *Adv. Sci.* 7, 1902443. doi:10.1002/advs.201902443

Wang, J., Tang, J., Zhang, P., Li, Y., Wang, J., Lai, Y., et al. (2012). Surface Modification of Magnesium Alloys Developed for Bioabsorbable Orthopedic Implants: A General Review. *J. Biomed. Mater. Res.* 100B, 1691–1701. doi:10.1002/jbm.b.32707

Wang, P., Liu, J., Shen, S., Li, Q., Luo, X., Xiong, P., et al. (2019b). *In Vitro* and *In Vivo* Studies on Two-step Alkali-Fluoride-Treated Mg-Zn-Y-Nd Alloy for Vascular Stent Application: Enhancement in Corrosion Resistance and Biocompatibility. *ACS Biomater. Sci. Eng.* 5, 3279–3292. doi:10.1021/acsbiomaterials.9b00140

Wang, T., Yang, G., Zhou, W., Hu, J., Jia, W., and Lu, W. (2019c). One-pot Hydrothermal Synthesis, *In Vitro* Biodegradation and Biocompatibility of Sr-Doped Nanorod/nanowire Hydroxyapatite Coatings on ZK60 Magnesium alloy. *J. Alloys Comp.* 799, 71–82. doi:10.1016/j.jallcom.2019.05.338

Wang, X., Wang, X., Wang, D., Zhao, M., and Han, F. (2018). A Novel Approach to Fabricate Zn Coating on Mg Foam through a Modified thermal Evaporation Technique. *J. Mater. Sci. Tech.* 34, 1558–1563. doi:10.1016/j.jmst.2017.12.019

Wang, Z.-X., Xu, L., Zhang, J.-W., Ye, F., Lv, W.-G., Xu, C., et al. (2020c). Preparation and Degradation Behavior of Composite Bio-Coating on ZK60 Magnesium Alloy Using Combined Micro-arc Oxidation and Electrophoresis Deposition. *Front. Mater.* 7. doi:10.3389/fmats.2020.00190

Wang, Z.-X., Zhang, J.-W., Ye, F., Lv, W.-G., Lu, S., Sun, L., et al. (2020d). Properties of Micro-arc Oxidation Coating Fabricated on Magnesium under Two Steps Current-Decreasing Mode. *Front. Mater.* 7. doi:10.3389/fmats.2020.00261

Witecka, A., Valet, S., Basista, M., and Boccaccini, A. R. (2021). Electrophoretically Deposited High Molecular Weight Chitosan/bioactive Glass Composite Coatings on WE43 Magnesium alloy. *Surf. Coat. Tech.* 418, 127232. doi:10.1016/j.surfcoat.2021.127232

Wu, T.-C., Ho, Y.-H., Joshi, S. S., Rajamure, R. S., and Dahotre, N. B. (2017). Microstructure and Corrosion Behavior of Laser Surface-Treated AZ31B Mg Bio-Implant Material. *Lasers Med. Sci.* 32, 797–803. doi:10.1007/s10103-017-2174-1

Wu, T.-C., Joshi, S. S., Ho, Y.-H., Pantawane, M. V., Sinha, S., and Dahotre, N. B. (2021). Microstructure and Surface Texture Driven Improvement in *In-Vitro* Response of Laser Surface Processed AZ31B Magnesium alloy. *J. Magnesium Alloys* 9, 1406–1418. doi:10.1016/j.jma.2020.11.002

Xi, W., Hegde, V., Zoller, S. D., Park, H. Y., Hart, C. M., Kondo, T., et al. (2021). Point-of-care Antimicrobial Coating Protects Orthopaedic Implants from Bacterial challenge. *Nat. Commun.* 12, 1–15. doi:10.1038/s41467-021-25383-z

Xi, Z., Wu, Y., Xiang, S., Sun, C., Wang, Y., Yu, H., et al. (2020). Corrosion Resistance and Biocompatibility Assessment of a Biodegradable Hydrothermal-Coated Mg-Zn-Ca Alloy: An *In Vitro* and *In Vivo* Study. *ACS Omega* 5, 4548–4557. doi:10.1021/acsomega.9b03889

Xie, J., Zhang, J., Liu, S., Li, Z., Zhang, L., Wu, R., et al. (2019). Hydrothermal Synthesis of Protective Coating on Mg alloy for Degradable Implant Applications. *Coatings* 9, 1–10. doi:10.3390/coatings9030160

Xiong, Y., Hu, X., Weng, Z., and Song, R. (2020). Stress Corrosion Resistance of Laser Shock Peening/Microarc Oxidation Reconstruction Layer Fabricated on

AZ80 Magnesium Alloy in Simulated Body Fluid. *J. Materi Eng. Perform.* 29, 5750–5756. doi:10.1007/s11665-020-05076-2

Yang, G., Chen, T., Feng, B., Weng, J., Duan, K., Wang, J., et al. (2019a). Improved Corrosion Resistance and Biocompatibility of Biodegradable Magnesium alloy by Coating Graphite Carbon Nitride (G-C3n4). *J. Alloys Comp.* 770, 823–830. doi:10.1016/j.jallcom.2018.08.180

Yang, Q., Yuan, W., Liu, X., Zheng, Y., Cui, Z., Yang, X., et al. (2017). Atomic Layer Deposited ZrO2 Nanofilm on Mg-Sr alloy for Enhanced Corrosion Resistance and Biocompatibility. *Acta Biomater.* 58, 515–526. doi:10.1016/j.actbio.2017.06.015

Yang, Y., Shi, Z., Cui, X., Liu, Y., Jin, G., Virtanen, S., et al. (2021). Preliminary Studies for One-step Fabrication of Metallic Iron-Based Coatings on Magnesium as Temporary Protection in Biodegradable Medical Application. *Front. Mater.* 8. doi:10.3389/fmats.2021.786650

Yang, Y., Zhou, J., Chen, Q., Detsch, R., Cui, X., Jin, G., et al. (2019b). *In Vitro* Osteocompatibility and Enhanced Biocorrosion Resistance of Diammonium Hydrogen Phosphate-Pretreated/Poly(ether Imide) Coatings on Magnesium for Orthopedic Application. *ACS Appl. Mater. Inter.* 11, 29667–29680. doi:10.1021/acsami.9b11073

Yao, H.-L., Hu, X.-Z., Yi, Z.-H., Xia, J., Tu, X.-Y., Li, S.-B., et al. (2021). Microstructure and Improved Anti-corrosion Properties of Cold-Sprayed Zn Coatings Fabricated by post Shot-Peening Process. *Surf. Coat. Tech.* 422, 127557. doi:10.1016/j.surfcoat.2021.127557

Yasakau, K. A., Bastos, A. C., Haffner, D., Quandt, E., Feyerabend, F., Ferreira, M. G. S., et al. (2021). Sacrificial protection of Mg-Based Resorbable Implant alloy by Magnetron Sputtered Mg5Gd alloy Coating: A Short-Term Study. *Corrosion Sci.* 189, 109590. doi:10.1016/j.corsci.2021.109590

Zaffora, A., Di Franco, F., Virtù, D., Carfì Pavia, F., Ghersi, G., Virtanen, S., et al. (2021). Tuning of the Mg Alloy AZ31 Anodizing Process for Biodegradable Implants. *ACS Appl. Mater. Inter.* 13, 12866–12876. doi:10.1021/acsami.0c22933

Zeng, R.-C., Cui, L.-y., Jiang, K., Liu, R., Zhao, B.-D., and Zheng, Y.-F. (2016). *In Vitro* Corrosion and Cytocompatibility of a Microarc Oxidation Coating and Poly(l-Lactic Acid) Composite Coating on Mg-1Li-1Ca Alloy for Orthopedic Implants. *ACS Appl. Mater. Inter.* 8, 10014–10028. doi:10.1021/acsami.6b00527

Zhang, C., Dong, Y., and Ye, C. (2021a). Recent Developments and Novel Applications of Laser Shock Peening: A Review. *Adv. Eng. Mater.* 23, 2001216–2001224. doi:10.1002/adem.202001216

Zhang, J., Guan, Y., Lin, W., and Gu, X. (2019a). Enhanced Mechanical Properties and Biocompatibility of Mg-Gd-Ca alloy by Laser Surface Processing. *Surf. Coat. Tech.* 362, 176–184. doi:10.1016/j.surfcoat.2019.01.063

Zhang, J., Zhang, B., Zhang, J., Lin, W., and Zhang, S. (2021b). Magnesium Promotes the Regeneration of the Peripheral Nerve. *Front. Cel Dev. Biol.* 9. doi:10.3389/fcell.2021.717854

Zhang, R., Zhou, X., Gao, H., Mankoci, S., Liu, Y., Sang, X., et al. (2018). The Effects of Laser Shock Peening on the Mechanical Properties and Biomedical Behavior of AZ31B Magnesium alloy. *Surf. Coat. Tech.* 339, 48–56. doi:10.1016/j.surfcoat.2018.02.009

Zhang, T. C., Zhang, K. M., Zou, J. X., Yan, P., Yang, H. Y., Song, L. X., et al. (2019b). Surface Microstructure and Property Modifications in a Mg-8Gd-3Y-0.5Zr Magnesium alloy Treated by High Current Pulsed Electron Beam. *J. Alloys Comp.* 788, 231–239. doi:10.1016/j.jallcom.2019.02.130

Zhang, Y., and Lin, T. (2019). Influence of Duty Cycle on Properties of the Superhydrophobic Coating on an Anodized Magnesium alloy Fabricated by Pulse Electrodeposition. *Colloids Surf. A: Physicochemical Eng. Aspects* 568, 43–50. doi:10.1016/j.colsurfa.2019.01.078

Zhang, Z.-Q., Wang, L., Zeng, M.-Q., Zeng, R.-C., Kannan, M. B., Lin, C.-G., et al. (2020). Biodegradation Behavior of Micro-arc Oxidation Coating on Magnesium alloy-from a Protein Perspective. *Bioactive Mater.* 5, 398–409. doi:10.1016/j.bioactmat.2020.03.005

Zhao, D., Witte, F., Lu, F., Wang, J., Li, J., and Qin, L. (2017). Current Status on Clinical Applications of Magnesium-Based Orthopaedic Implants: A Review from Clinical Translational Perspective. *Biomaterials* 112, 287–302. doi:10.1016/j.biomaterials.2016.10.017

Zhao, X., Jing, W., Yun, Z., Tong, X., Li, Z., Yu, J., et al. (2021). An Experimental Study on Stress-Shielding Effects of Locked Compression Plates in Fixing Intact Dog Femur. *J. Orthop. Surg. Res.* 16, 1–11. doi:10.1186/s13018-021-02238-3

Zhao, Y.-B., Liu, H.-P., Li, C.-Y., Chen, Y., Li, S.-Q., Zeng, R.-C., et al. (2018). Corrosion Resistance and Adhesion Strength of a Spin-Assisted Layer-By-Layer Assembled Coating on AZ31 Magnesium alloy. *Appl. Surf. Sci.* 434, 787–795. doi:10.1016/j.apsusc.2017.11.012

Zhou, H., Li, J., Li, J., Ruan, Q., Peng, X., Li, S., et al. (2021). A Composite Coating with Physical Interlocking and Chemical Bonding on WE43 Magnesium alloy for Corrosion protection and Cytocompatibility Enhancement. *Surf. Coat. Tech.* 412, 127078. doi:10.1016/j.surfcoat.2021.127078

Zhou, J., Li, K., Wang, B., and Ai, F. (2020). Nano-hydroxyapatite/ZnO Coating Prepared on a Biodegradable Mg-Zn-Ca Bulk Metallic Glass by One-step Hydrothermal Method in Acid Situation. *Ceramics Int.* 46, 6958–6964. doi:10.1016/j.ceramint.2019.11.074

Zou, X., Zhang, L., Wang, Z., and Luo, Y. (2016). Mechanisms of the Antimicrobial Activities of Graphene Materials. *J. Am. Chem. Soc.* 138, 2064–2077. doi:10.1021/jacs.5b11411

Conflict of Interest: The authors declare that the research was conducted in the absence of any commercial or financial relationships that could be construed as a potential conflict of interest.

Publisher's Note: All claims expressed in this article are solely those of the authors and do not necessarily represent those of their affiliated organizations, or those of the publisher, the editors, and the reviewers. Any product that may be evaluated in this article, or claim that may be made by its manufacturer, is not guaranteed or endorsed by the publisher.